

Electronic Supplementary Information

A unique water soluble probe for measuring the cardiac marker homocysteine and its clinical validation

Snehasish Debnath,^{a,b} Ratish R. Nair,^{a,b} Riya Ghosh,^{a,b} Gaddam Kiranmai,^c Narsini

Radhakishan,^d Narayana Nagesh,^{*c} and Pabitra B. Chatterjee^{*a,b}

^aAnalytical & Environmental Science Division and Centralized Instrument Facility,

CSIR-CSMCRI, G. B. Marg, Bhavnagar, Gujarat, India.

^bAcademy of Scientific and Innovative Research (AcSIR), Ghaziabad 201002, India.

^cMedical Biotechnology Complex, CSIR-CCMB, ANNEXE II, Hyderabad, Telangana, India.

^dDepartment of Biochemistry, Nizam's Institute of Medical Sciences,

Punjagutta, Hyderabad, Telangana, India.

*Corresponding author: pbchatterjee@csmcri.res.in

nagesh@ccmb.res.in

Experimental Section

Materials and Physical Measurements

7-Hydroxy-4-methylcoumarin, 7-hydroxycoumarin, N,N-dimethylethylenediamine, N,N-diethylethylenediamine, hexamine, glacial acetic acid, glutathione, ATP (adenosine triphosphate), ADP (adenosine diphosphate), AMP (adenosine monophosphate), HSA (human serum albumin), L-dehydroascorbic acid (DHA), CORM-3 (CO releasing molecule), cytochrome-C, potassium dioxide, spermine, spermidine, sodium nitroprusside dihydrate, nitrosyl tetrafluoroborate, 2,2'-azobis(2-methylpropionamide)dihydrochloride, copper nitrate trihydrate, and other chemicals were procured from Sigma Aldrich and TCI. L-amino acids (Cys, Phe, Ala, Pro, Thr, His, Ile, Arg, Lys, Val, Leu, Met, Gln, Ser, Gly, Asn, Hyp, Asp, and Glu) were procured from Sisco Research Laboratories (SRL) Pvt. Ltd. India. All solvents were acquired from Finar and Spectrochem Pvt. Ltd. India and were used without any further purification. IR spectra were recorded using Perkin–Elmer GX FTIR spectrometer using KBr pellet in the region $450\text{--}4000\text{ cm}^{-1}$. Elemental analyses (C, H, and N) were performed on an Elementar Vario MICRO CUBE analyser. JEOL Resonance ECZR 600 MHz spectrometer and FT-NMR (500 MHz) Advance II Bruker Labscape AV500 Essential were used for ^1H and ^{13}C NMR spectra. For ^1H NMR and ^{13}C NMR experiments, TMS was used as internal standard. The UV-vis spectra were recorded with Shimadzu 3600 UV-Vis-NIR spectrophotometer and Varian Cary-500 UV-Vis spectrophotometer. Samples for absorption measurement were taken in 1 cm thick quartz cuvette. Fluorescence experiments were performed on Fluorolog FL 1065 Horiba Jobin Yvon Spectrometer instrument and Edinburgh instrument Xe 900 (μF 920H). Fluorescence measurements were performed in 10 mm quartz cuvette. pH of the solutions were measured using Thermo Scientific Orion Versa-star Advanced Electrochemistry meter at 298 K. The ESI-MS was measured on Micromass Q-ToF microTM and Agilent technologies

6545 Q–TOF LCMS. The melting points of the ligands were measured using a Mettler-Toledo FP-62 instrument. Single crystal X-ray diffraction analysis was performed using BRUKER SMART APEX (CCD) diffractometer. HPLC analysis was performed using reverse-phase (RP) HPLC, carried out by C18 column (100 Å; packed with mesh size 5 µm particles) of 150 mm length and 4.6 mm internal diameter. Edinburgh instrument OB 920 spectrofluorometer was used for performing lifetime experiments (TCSPC). Freiberg Instrument Miniscope MS-5000 bench top EPR/ESR X-band spectrometer with 9.8 GHz microwave frequency was used for performing EPR experiments. EPR experiments were conducted at 30 °C in water using 10 mW microwave power and 0.2 mT modulation. Molar conductivity of the complex was measured using Thermoscientific Orion Star A212 conductivity meter at 25 °C. In order to proceed with clinical investigation, ethical clearance from the Institute's Ethical Clearance Committee (CCMB-IEC) has been obtained to collect blood samples from cardiac patients and healthy volunteers as well.

Single Crystal X-ray Crystallography

Diffraction quality single crystal of HL₁ (block, brown, 0.6 x 0.38 x 0.3 mm³), HL₃ (plates, yellow, 0.234 x 0.046 x 0.012 mm³), HL₄ (block, brown, 0.523 x 0.502 x 0.490 mm³), and compound 1 (rod, green, 0.640 x 0.162 x 0.074 mm³) with suitable dimension were selected for data collection. Intensity data of HL₁, HL₃, HL₄, and complex 1 were acquired at 100(2) K, 117(2) K, 113(2) K, and 111(2) K, respectively. A BRUKER SMART APEX diffractometer equipped with a CCD detector with MoK α radiation ($\lambda=0.71073$ Å) source was used for the data collection. Data collection was performed using ϕ and ω scan and no crystal decay was observed during the data collection. Summary of crystallographic data are compiled in Table S2 and S3. Accurate cell parameters and orientation matrices of the crystals were acquired from setting angles in the ranges $2.697 \leq \theta \leq 31.51^\circ$ containing 4351 reflections for HL₁, $2.55 \leq \theta \leq 30.56^\circ$

containing 3823 reflections for HL₃, $2.47 \leq \theta \leq 28.27^\circ$ containing 7164 reflections for HL₄, and $2.42 \leq \theta \leq 30.59^\circ$ containing 5371 reflections for 1. After the data collection, empirical absorption corrections were carried out using the multi-scan and SADABS software.¹ For data collection and refinement, Bruker SMART software package was used. Bruker SAINT was employed for data integration and reduction.² The structures were solved by conventional direct methods and refined on F² by a full matrix least squares with SHELXTL.³ All non-hydrogen atoms were refined anisotropically based on all data minimizing $wR = [\sum[w((F_0^2 - F_c^2)^2)]^{1/2}$, $R = \sum||F_0| - |F_c||/\sum|F_0|$ and $S = [\sum[w((F_0^2 - F_c^2)^2)]/(n-p)]^{1/2}$. SHELXL-97 and SHELXL-2014 were used for structure solution and structure refinement. ORTEP-3 was used to draw crystallographic diagram at 50 % probability level.⁴

General Procedure for Solution State Fluorescence Selectivity Studies

1 mM stock solutions of different amino acids (Hcy, Cys, Phe, Ala, Pro, Thr, His, Ile, Arg, Lys, Val, Leu, Met, Gln, Ser, Gly, Asn, Hyp, Asp, and Glu) and GSH and 250 μ M stock solutions of ATP, ADP, AMP, HSA, DHA, CORM-3 (CO releasing molecule), cytochrome-C, potassium dioxide (superoxide radical), spermine (biogenic amine), spermidine (biogenic amine), sodium nitroprusside dehydrate (NO source), nitrosyl tetrafluoroborate (NO⁺), 2,2'-azobis(2-methylpropionamide)dihydrochloride (ROO[•]), sodium nitrate, and sodium nitrite, were prepared in ultrapure water. 40 μ M aqueous stock solutions of compounds 1-4 were prepared in HEPES buffer (10 mM, pH = 7.4). Fluorescence spectrum was measured after addition of 1 mL of respective analyte to 1 mL of probe's solution. The mixture was incubated for ca. 30 min. The excitation was set at $\lambda_{ex} = 370$ nm. Fluorescence measurement was performed in a 10 mm quartz cuvette. For comparison, control data were collected under identical conditions with blank solutions of 1-4 containing no Hcy.

General Procedure for Fluorescence Titration Experiments

For emission based titration, variable concentrations of Hcy was treated with 20 μM (100 % water) solutions of 1-4 in aqueous HEPES solution (10 mM, pH = 7.4). The concentration of the probe was kept constant at 20 μM . The values generated from the titration plots were further used to calculate binding constants between the analyte and probe using non-linear curve fitting equation (shown below) in which F_0 and F denote fluorescence intensities of 1-4 at 439/445 nm without and with Hcy, respectively.

$$F = F_0 + \frac{F_{max} - F_0}{2} \left\{ \left(1 + \frac{[M]}{C_L} + \frac{1}{C_L K} \right) - \sqrt{\left(1 + \frac{[M]}{C_L} + \frac{1}{C_L K} \right)^2 - 4 * \frac{[M]}{C_L}} \right\}$$

Limit of detection of Hcy using compound 1-4 was also obtained by the linear fitting of the titration points from the graph $[(F-F_0)/(F_\infty - F_0)]$ vs. $\log[\text{Hcy}]$.⁵

Time Correlated Single Photon Counting (TCSPC) Experiments

The time resolved fluorescence decay of the ligands HL₁-HL₄ and their Cu complexes, in presence and absence of Hcy, were performed by time-correlated single-photon counting (TCSPC) technique using Edinburgh instruments OB 920 fluorescence spectrophotometer equipped with a pulsed diode laser (Laser – EPLED-375 nm) as excitation source. Fluorescence excited state lifetime was measured by plotting fluorescence decay as a function of time (t), which enables the determination of fluorescence decay components. For lifetime measurements, fluorescence decay curve was analysed by a single exponential iterative fitting program using a software package provided by the Edinburgh Instrument.

Quantum Yield Measurement

For the determination of quantum efficiency of the compounds (before and after the addition of Hcy), anthracene ($\Phi_{\text{std}} = 0.27$) in ethanol solution was used as a standard. The quantum

yields were calculated according to the equation shown below.⁶ I_{sample} and I_{std} are the integrated fluorescence intensities of the sample and standard, respectively. A_{std} and A_{sample} are the absorbance values at the excitation wavelength of the standard and test sample, respectively. n_{sample} and n_{std} are the respective refractive indices of the sample and standard, respectively.

$$\Phi_{\text{sample}} = \Phi_{\text{std}} \times (I_{\text{sample}} / I_{\text{std}}) \times (A_{\text{std}} / A_{\text{sample}}) \times (n_{\text{sample}}^2 / n_{\text{std}}^2)$$

Procedure for HPLC Experiments

HPLC analysis was performed using reverse-phase (RP) HPLC using a C18 column (100 Å; packed with mesh size 5 µm particles) of 150 mm length and 4.6 mm internal diameter. Separations were made using mobile phase consisting of trichloroacetic acid buffer (pH = 2.3-2.5) and HPLC grade methanol in the ratio of 9:1. All the reagent solutions, buffers, and eluents were prepared using double distilled water. All liquids used for the HPLC analysis were further filtered through 0.2 µm membrane. The applied gradient elutant was pumped at 0.5 ml/min at 27 °C. The flow rate of the mobile phase was adjusted to 0.5 mL/min at 30 °C. The auto sampler injected 40 µL aliquot of each final solution. The UV detector was set at 312 nm as reported in the literature.⁷

The HPLC method, used in the present assay, was based on pre-column derivatization of Hcy using 2-chloro-1-methylpyridinium iodide (CMPI) as derivatizing, as well as UV labelling agent. Initially, a stock solution of 1 mM Hcy was prepared and further diluted to various concentrations. In a similar manner, 0.1 M stock solution of CMPI was also prepared. The internal standard cysteine-CPPI (2-chloro-1-methylpyridinium iodide) derivative was prepared as reported in the literature.⁷ To 500 µL of variable Hcy concentrations, 500 µL of 8.2 pH Tris buffer were added, followed by the addition of 50 µL 0.1 M CMPI solutions. The

aliquots were vortexed vigorously for several minutes and kept at room temperature for 30 minutes. Thus, Hcy-CMPI formed after the reaction was UV active and can be analysed by the UV detector at 312 nm in the HPLC technique. After derivatization, 25 μ L of 0.025 mM IS solutions were added to each sample. Afterwards, the solutions were further filtered through 0.2 μ m membrane and used for HPLC experiments.

Experimental Protocol and Reagents for Immunoassay

The chemiluminescence immunoassay (ICL) assay was carried out using ADVIA Centaur XP (Siemens, Germany) following the instructions supplied by the manufacturer. The assay was ran on an ADVIA Centaur XP. Calibrators manufactured by Siemens Healthineers as part of the test kit was also used. Among the participants, 25 % were healthy controls and 75 % were cardiac patients. After arresting the release of free Hcy from the erythrocytes, blood samples were centrifuged to separate plasma. To the plasma samples, appropriate quantity of dithiothreitol was added to release Hcy from its bound forms. Next, 40 μ M of 1 was added to the plasma sample and mixed thoroughly at room temperature for further investigation. Free Hcy was then converted to S-adenosylhomocysteine (SAH) by an enzyme reagent. Converted SAH from the patient is covalently coupled to paramagnetic particle in the solid phase for a limited amount of acridinium ester-labelled anti-SAH in the Lite reagent. Lite reagent, monoclonal mouse anti-SAH antibody (\approx 0.4 μ g/mL) labelled with acridinium ester in phosphate buffer with bovine serum albumin and preservatives; solid phase SAH (\approx 2.1 μ g/mL) covalently coupled to paramagnetic particle in phosphate buffer with bovine serum albumin and preservatives. Enzyme reagent (bovine derived S-adenosylhomocysteine hydrolase enzyme, \approx 60 mU/mL) in TRIS buffer with preservatives; reducing reagent dithiothreitol (DTT, \approx 1.5 mg/mL) in citrate buffer with preservatives; Hcy diluent (phosphate

buffer with bovine gamma globulin and preservatives) were purchased from Siemens Healthineers.

The ADVIA Centaur XP automatically performs the following steps to get the Hcy levels in the patient plasma.

- Dispense 10 μ L of sample into the cuvette,
- Dispense 50 μ L of reducing reagent and incubate it for 3 min at 37 $^{\circ}$ C,
- Dispense 50 μ L of enzyme reagent and incubate it for 2.5 min at 37 $^{\circ}$ C,
- Dispense 250 μ L of solid phase and incubate the mixture for 2.5 min at 37 $^{\circ}$ C,
- Dispense 100 μ L of the Lite reagent and incubate it for 2.5 min at 37 $^{\circ}$ C,
- Separate, aspirates, and washes the cuvettes with reagent water,
- Dispenses 300 μ L each of acid reagent and base reagent to initiate the chemiluminescent reaction,
- Report the results according to the selected option.

An inverse relationship exists between the amount of Hcy present in the patient sample and quantity of relative light units (RLUs) detected by the system. A separate calibration plot has been generated for the plasma samples.

Experimental Procedure for MTT Assay:

The cytotoxicity studies of **1** and its ternary iminocoumarin-Cu(I)-Hcy complex have been evaluated using A549 cell lines (human lung cancer cell lines) by MTT assay. Cytotoxicities were determined by measuring the *in-vitro* growth inhibition of A549 cell lines in 96-well plates. A549 cell lines were grown in Dulbecco's Modified Eagle's Medium (DMEM) with 10 % Fetal Bovine Serum (FBS) (20 % FBS for Gibco) and 1 % penicillin-streptomycin antibiotic

solution. The cells were seeded (4×10^3 cells / well (100 μ L)) in 96 well plates and incubated in CO₂ incubator for 24 h and were treated with compound 1 and fixed concentration of Hcy. The media was removed and 50 μ L of serum free media and 50 μ L of MTT reagent (i.e. 3-(4,5-dimethylthiazol-2-yl)-2,5-diphenyl tetrazolium bromide, 5 mg/ml) was added in each well and incubated at 37 °C for 3 h. Later, the media was removed and 150 μ L of DMSO was added to dissolve the formazan crystals. The absorbance was noted using a multimode ELISA reader at 570 nm. The results were evaluated using GraphPad Prism 6 software.

General synthesis of HL₁–HL₄

7-Hydroxy-4-methyl-2-oxo-2H-chromene-8-carbaldehyde (CA1) and 7-Hydroxy-2-oxo-2H-chromene-8-carbaldehyde (CA2) were prepared from the Duff's reaction, following the procedure described by Mie Kamoto et al.⁸ A mixture of CA1 (204 mg, 1 mmol) or CA2 (190 mg, 1 mmol) with N,N-dialkylethylenediamine (1 mmol) in 1:1 stoichiometry was taken in a round bottom flask and 15 mL of methanol was added to this mixture. The mixture was refluxed under stirring condition for 3-4 h. The progress of the reaction was monitored by TLC. After completion of the reaction, yellow solid was obtained by evaporating the solvent under reduced pressure using rotary evaporator. Further trituration with diethyl ether, solid ligand was collected and air dried. Recrystallization from diethyl ether resulted the crystalline product.

HL₁

Yield: 68 % (recrystallized). MP: 157 °C. ¹H NMR (CDCl₃, 600 MHz, δ ppm) = 14.83 (s, 1H, Phenolic O-H), 8.90 (s, 1H), 7.47 (d, 1H, J=9 Hz), 6.72 (d, 1H, J=9 Hz), 6.00 (s, 1H), 3.72 (t, 2H, J=6 Hz), 2.64 (t, 2H, J=6 Hz), 2.36 (s, 3H), 2.31 (s, 6H). ¹³C NMR (CDCl₃, 150 MHz, δ ppm) = 19.04, 45.63, 52.67, 59.06, 104.89, 108.08, 109.05, 118.43, 130.02, 153.90, 155.44, 160.35,

160.82, 174.05. Anal. Calcd for $C_{15}H_{18}N_2O_3$: C, 65.68; H, 6.61; N, 10.21. Found: C, 64.13; H, 6.4; N, 9.9. ESI-MS (+ive, m/Z): 275.14 [M+H⁺]. Selected IR bands (cm^{-1}): 3435, 2941, 2770, 1723, 1636, 1578, 1504, 1436, 1424, 1340, 1245, 1174, 1057, 834. UV-vis (H_2O) [λ_{max} , nm (ϵ , $Lmol^{-1}cm^{-1}$): 350 (36000) and 277 (17400)].

HL₂

Yield: 62 % (recrystallized). MP: 107 °C. ¹H NMR ($CDCl_3$, 600 MHz, δ ppm) = 8.85 (s, 1H), 7.46 (d, 1H, J=9.6 Hz), 6.70 (d, 1H, J=9 Hz), 5.99 (s, 1H), 3.66 (t, 2H, J=6 Hz), 2.76 (t, 2H, J=6 Hz), 2.59 (q, 4H, J=7.2 Hz), 2.36 (s, 3H), 1.03 (t, 6H, J=7.2 Hz). ¹³C NMR ($CDCl_3$, 150 MHz, δ ppm) = 12.03, 18.99, 47.31, 52.42, 52.70, 104.49, 107.46, 108.61, 119.08, 130.18, 153.94, 155.70, 160.25, 160.87, 175.42. Anal. Calcd for $C_{17}H_{22}N_2O_3$: C, 67.53; H, 7.33; N, 9.26. Found: C, 66.47; H, 7.52; N, 9.17. ESI-MS (+ive, m/Z): 303.17 [M+H⁺]. Selected IR bands (cm^{-1}): 3431, 2967, 2931, 2864, 2798, 1735, 1720, 1644, 1585, 1507, 1433, 1380, 1184, 1066, 829. UV-vis (H_2O) [λ_{max} , nm (ϵ , $Lmol^{-1}cm^{-1}$): 350 (40235) and 279 (20660)].

HL₃

Yield: 68 % (recrystallized). MP: 108 °C. ¹H NMR ($CDCl_3$, 600 MHz, δ ppm) = 14.74 (s, 1H, Phenolic O-H), 8.86 (s, 1H), 7.56 (d, 1H, J= 9. Hz), 7.31 (d, 1H, J= 9 Hz), 6.69 (d, 1H, J= 9 Hz), 6.11 (d, 1H, J= 9.6 Hz), 3.72 (t, 2H, J= 6 Hz), 2.65 (t, 2H, J= 6 Hz), 2.31 (s, 6H). ¹³C NMR ($CDCl_3$, 150 MHz, δ ppm) = 45.62, 52.28, 58.97, 104.79, 107.05, 109.59, 119.21, 133.43, 144.54, 156.40, 159.89, 160.90, 174.99. Anal. Calcd for $C_{14}H_{16}N_2O_3$: C, 64.60; H, 6.20; N, 10.76. Found: C, 64.13; H, 6.21; N, 10.59. ESI-MS (+ive, m/Z): 261.12 [M+H⁺]. Selected IR bands (cm^{-1}): 3435, 2944, 2817, 2766, 1720, 1641, 1581, 1514, 1465, 1430, 1348, 1232, 1186, 1103, 994, 824. UV-vis (H_2O) [λ_{max} , nm (ϵ , $Lmol^{-1}cm^{-1}$): 353 (27250) and 277 (14200)].

HL₄

Yield: 62 % (recrystallized). MP: 102 °C. ¹H NMR (CDCl₃, 600 MHz, δ ppm) = 14.60 (s, 1H, Phenolic O-H), 8.81 (s, 1H), 7.54 (d, 1H, J=9.6 Hz), 7.30 (d, 1H, J=9 Hz), 6.60 (d, 1H, J= 9 Hz), 6.09 (d, 1H, J= 9.6 Hz), 3.66 (t, 2H, J=6 Hz), 2.76 (t, 2H, J= 6 Hz), 2.59 (q, 4H, J= 7.2 Hz), 1.03 (t, 6H, J=7.2 Hz). ¹³C NMR (CDCl₃, 150 MHz, δ ppm) =12.11, 47.36, 52.16, 52.75, 104.46, 106.52, 109.15, 119.88, 133.62, 144.60, 156.74, 159.84, 160.98, 176.35. Anal. Calcd for C₁₆H₂₀N₂O₃: C, 66.65; H, 6.99; N, 9.72. Found: C, 65.47; H, 7.22; N, 9.47. ESI-MS (+ive, m/Z): 289.16 [M+H⁺]. Selected IR bands (cm⁻¹): 3419, 2964, 2802, 1736, 1720, 1641, 1618, 1584, 1503, 1438, 1349, 1246, 1138, 1092, 981, 826. UV-vis (H₂O) [λ_{max} , nm (ϵ , Lmol⁻¹cm⁻¹): 356 (21100) and 274 (8050).

General synthesis of the Cu complexes 1-4

Compounds 1-4 were synthesized by reacting stoichiometric amount of the respective ligands (HL₁ - HL₄) with copper nitrate in methanol solution. A mixture of copper nitrate trihydrate (241.6 mg, 1 mmol) and the iminocoumarin ligand (HL₁ - HL₄) (1 mmol) in 1:1 stoichiometry was taken in a round bottom flask and 30 mL methanol solution was added to this mixture. The mixture was refluxed under stirring for ca. 3-4 h. Green solid was obtained as precipitates after evaporating half of the solvent using rotary evaporator, which was further recrystallized from acetonitrile to obtain the pure solid.

[Cu(L₁)(H₂O)₂]NO₃ (1)

Yield: 60 % (recrystallized). Selected IR bands (cm⁻¹): 3432, 2926, 1720, 1628, 1583, 1526, 1469, 1406, 1381, 1280, 1184, 1101, 1057, 1012, 836 and 775. Anal. Calcd for C₁₅H₂₁N₃O₈Cu: C, 41.43; H, 4.87; N, 9.66. Found: C, 41.11; H, 5.02; N, 9.91. UV-vis (H₂O) [λ_{max} , nm (ϵ , Lmol⁻¹cm⁻¹): 410 (11050), 365 (21100), 332 (33000), 289 (36200), 257 (38100), 215 (67200), 625

nm (d-d band, ϵ , $160 \text{ Lmol}^{-1}\text{cm}^{-1}$). Molar conductivity of the compound infers 1:1 electrolytic nature.

[Cu(L₂)(H₂O)₂]NO₃ (2)

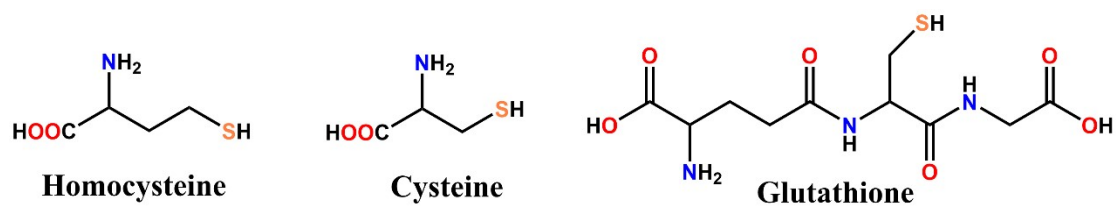
Yield: 52 % (recrystallized). Selected IR bands (cm^{-1}): 3423, 2976, 2938, 1730, 1630, 1581, 1530, 1476, 1404, 1338, 1284, 1189, 1100, 1060, 1011, 840, 772 and 740. Anal. Calcd for $\text{C}_{17}\text{H}_{25}\text{N}_3\text{O}_8\text{Cu}$: C, 44.11; H, 5.44; N, 9.08. Found: C, 44.73; H, 5.32; N, 9.11. UV-vis (H_2O) [λ_{max} , nm (ϵ , $\text{Lmol}^{-1}\text{cm}^{-1}$): 418 (4800), 364 (14050), 339 (18500), 281 (18900), 211 (52450).

[Cu(L₃)(H₂O)₂]NO₃ (3)

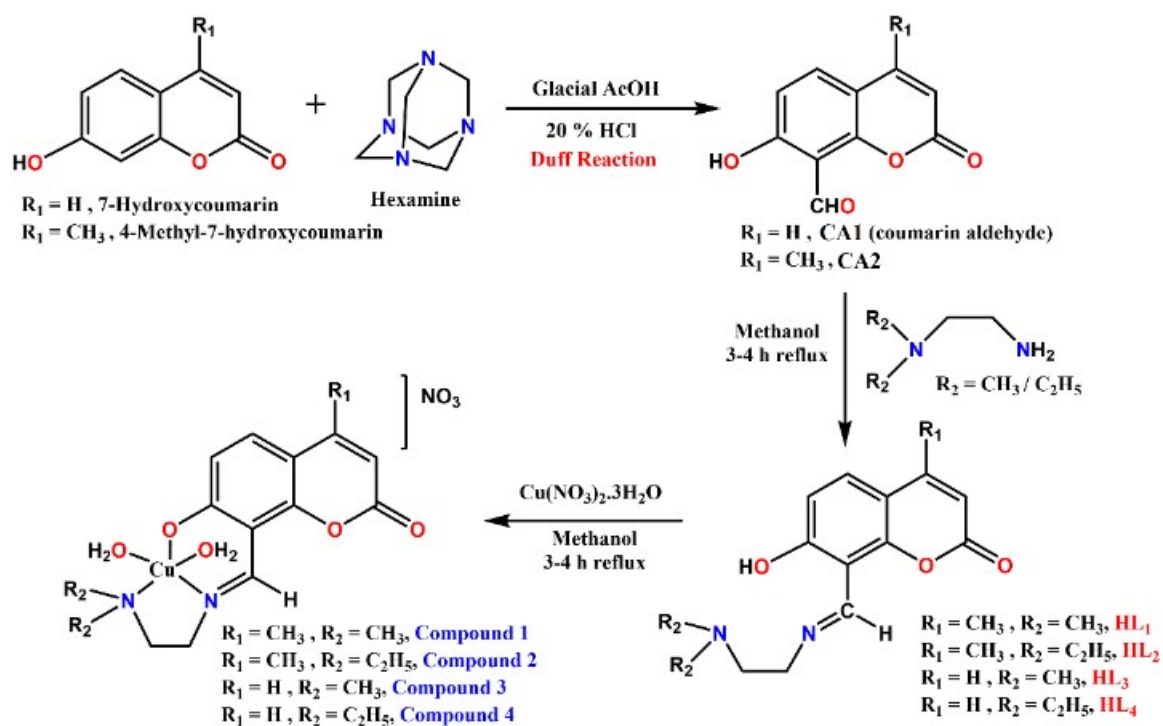
Yield: 51 % (recrystallized). Selected IR bands (cm^{-1}): 3414, 3050, 2920, 1718, 1625, 1584, 1525, 1469, 1402, 1383, 1355, 1287, 1080, 1009, 838, 773. Anal. Calcd for $\text{C}_{14}\text{H}_{19}\text{N}_3\text{O}_8\text{Cu}$: C, 39.95; H, 4.55; N, 9.98. Found: C, 40.39; H, 4.63; N, 10.11. UV-vis (H_2O) [λ_{max} , nm (ϵ , $\text{Lmol}^{-1}\text{cm}^{-1}$): 374 (18450), 350 (26800), 268 (23600), 248 (23000), 212 (62150).

[Cu(L₄)(H₂O)₂]NO₃ (4)

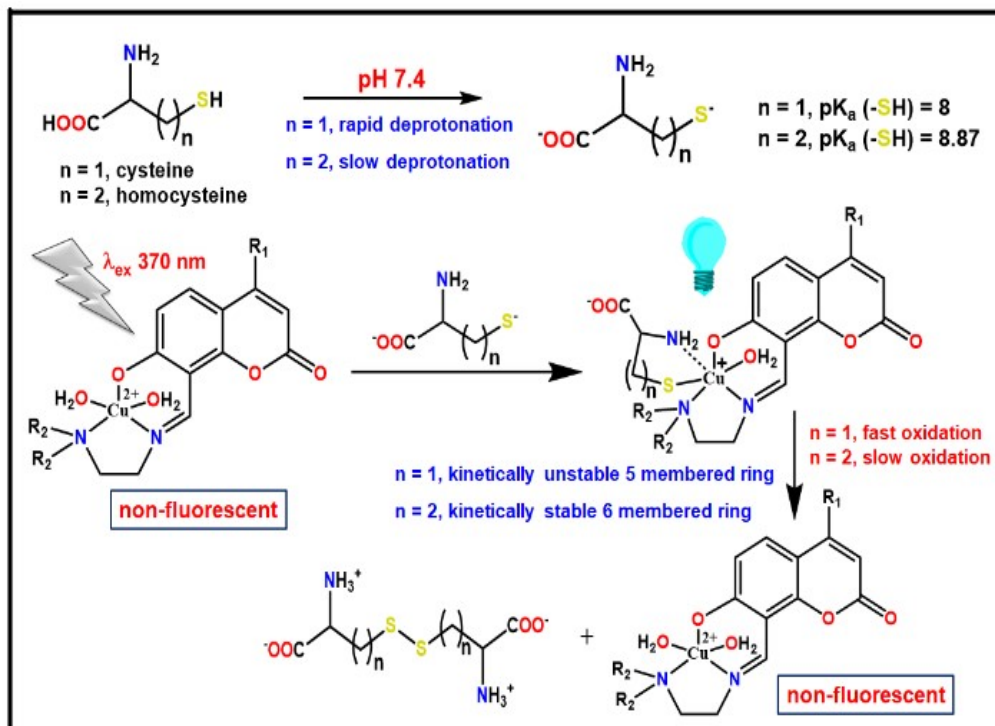
Yield: 52 % (recrystallized). Selected IR bands (cm^{-1}): 3428, 3061, 2975, 2920, 1732, 1628, 1587, 1525, 1469, 1411, 1386, 1285, 1072, 1009, 832, 773. Anal. Calcd for $\text{C}_{16}\text{H}_{23}\text{N}_3\text{O}_8\text{Cu}$: C, 42.81; H, 5.16; N, 9.36. Found: C, 42.57; H, 5.23; N, 9.11. UV-vis (H_2O) [λ_{max} , nm (ϵ , $\text{Lmol}^{-1}\text{cm}^{-1}$): 432 (8400), 372 (14400), 347 (20350), 273 (20150), 244 (17800), 211 (47950).



Scheme S1. Molecular structures of different biothiols.



Scheme S2. Synthetic protocol for the preparation of the copper compounds 1-4.



Scheme S3. Proposed mechanism of interaction between compounds 1-4 and biothiols cysteine (Cys, top) and homocysteine (Hcy, bottom) at physiological pH revealing the preferential selectivity of the compounds for Hcy.

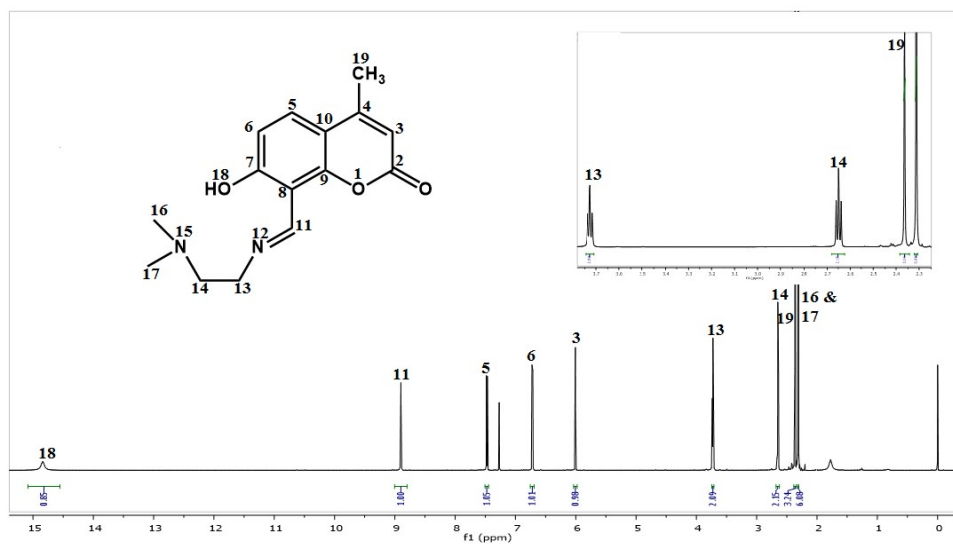


Fig. S1. ^1H NMR spectrum of HL_1 in CDCl_3 .

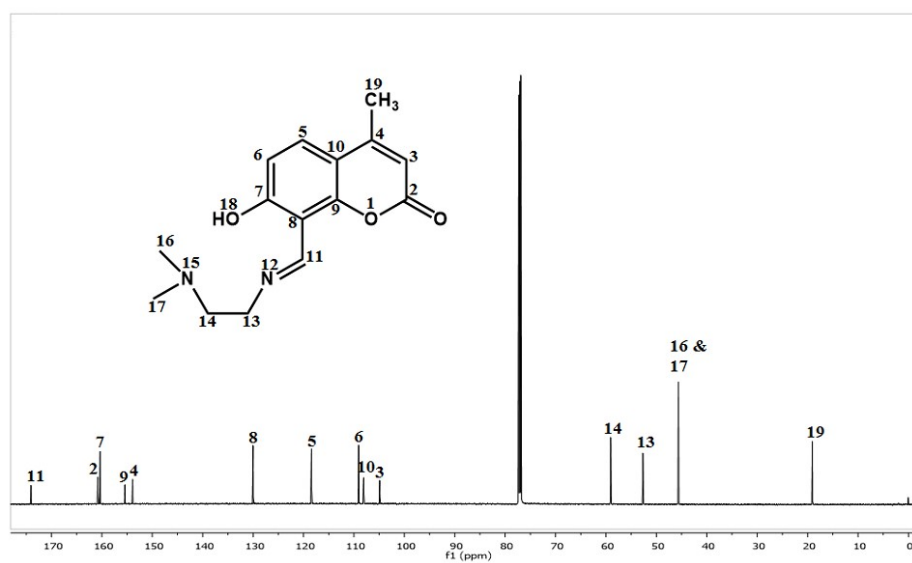


Fig. S2. ^{13}C NMR spectrum of HL_1 in CDCl_3 .

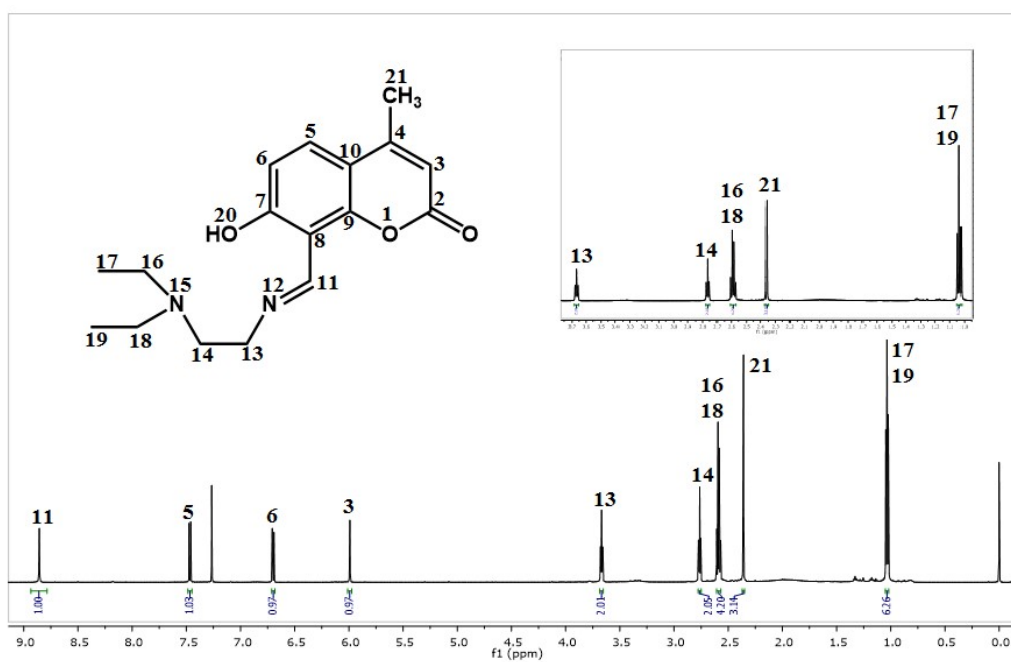


Fig. S3. ^1H NMR spectrum of HL_2 in CDCl_3 .

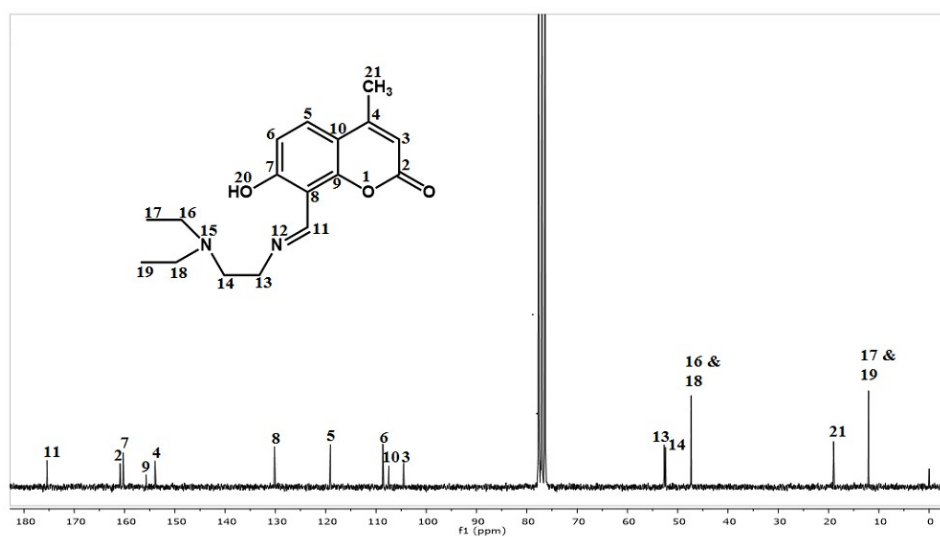


Fig. S4. ^{13}C NMR spectrum of HL_2 in CDCl_3 .

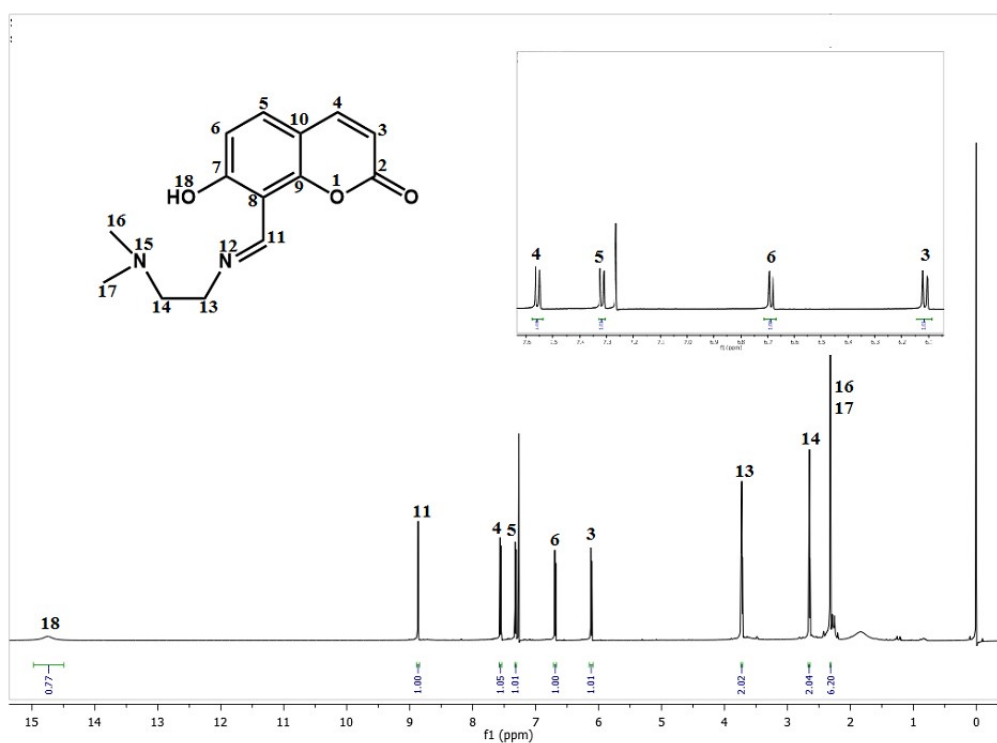


Fig. S5. ¹H NMR spectrum of HL₃ in CDCl₃.

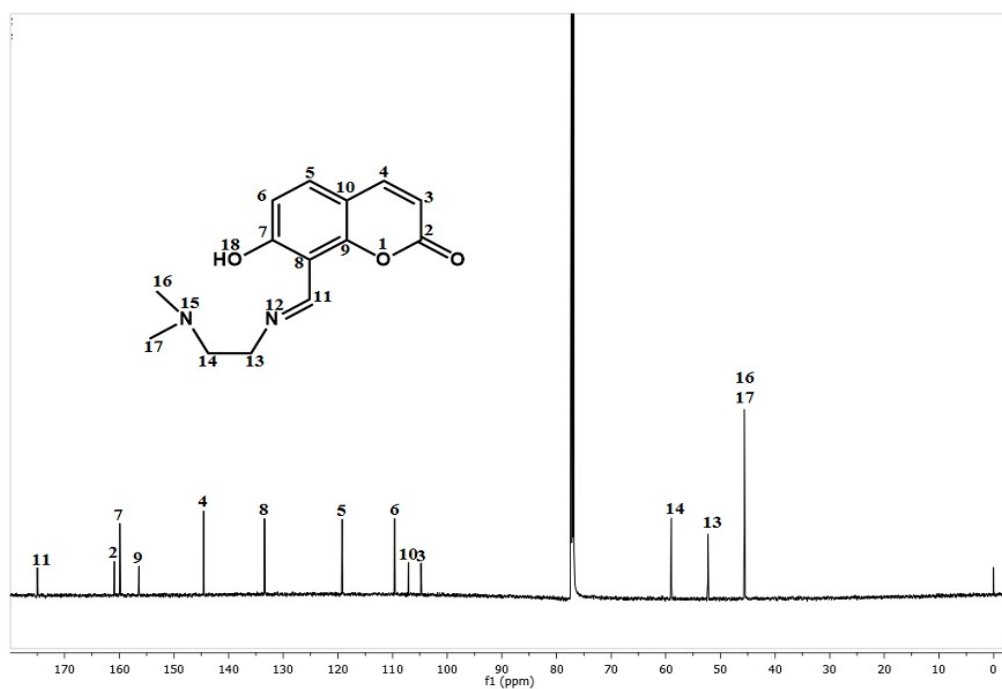


Fig. S6. ¹³C NMR spectrum of HL₃ in CDCl₃.

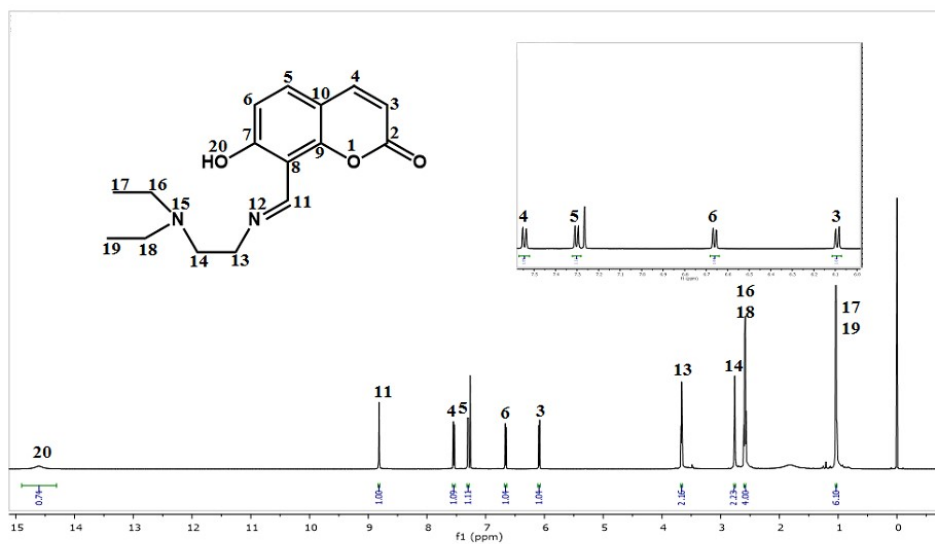


Fig. S7. ^1H NMR spectrum of HL₄ in CDCl_3 .

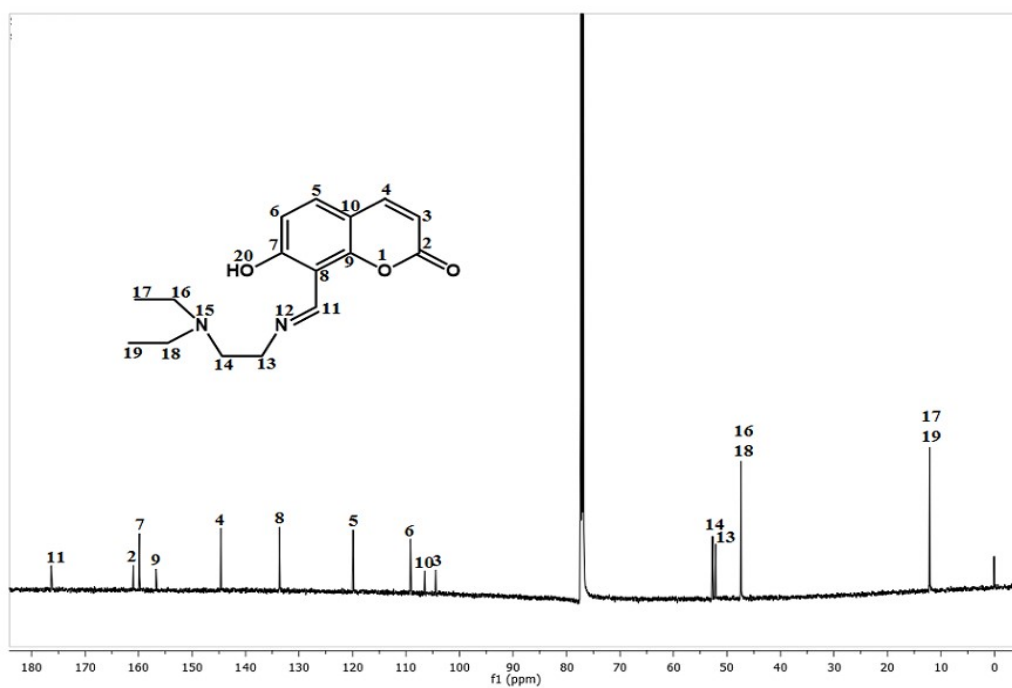


Fig. S8. ^{13}C NMR spectrum of HL₄ in CDCl_3 .

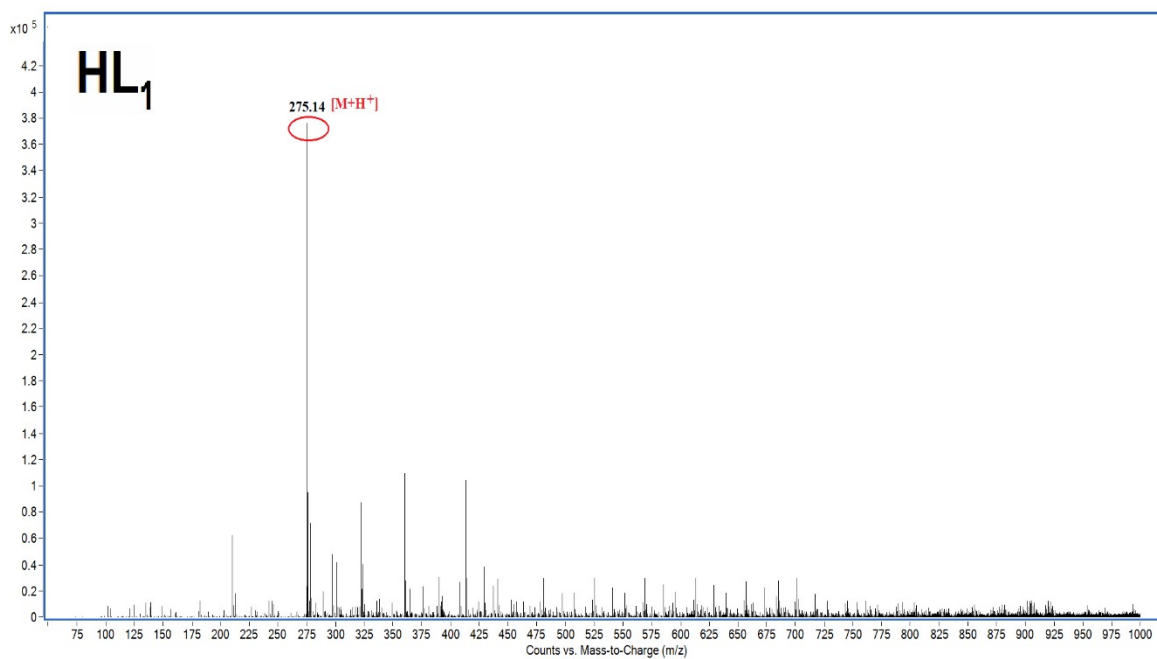


Fig. S9. ESI-MS spectrum of HL₁.

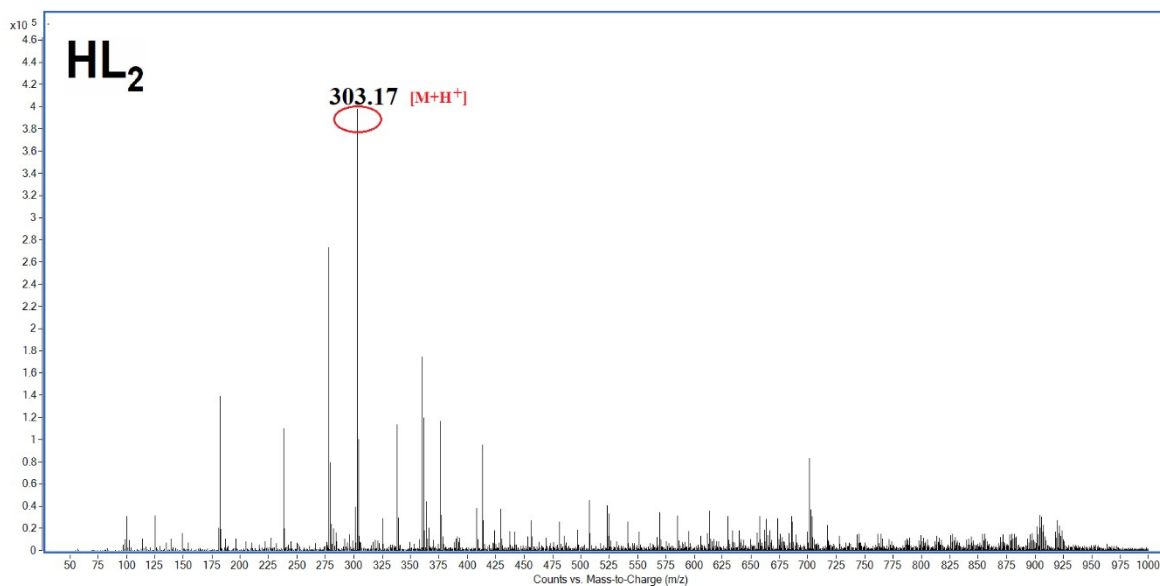


Fig. S10. ESI-MS spectrum of HL₂.

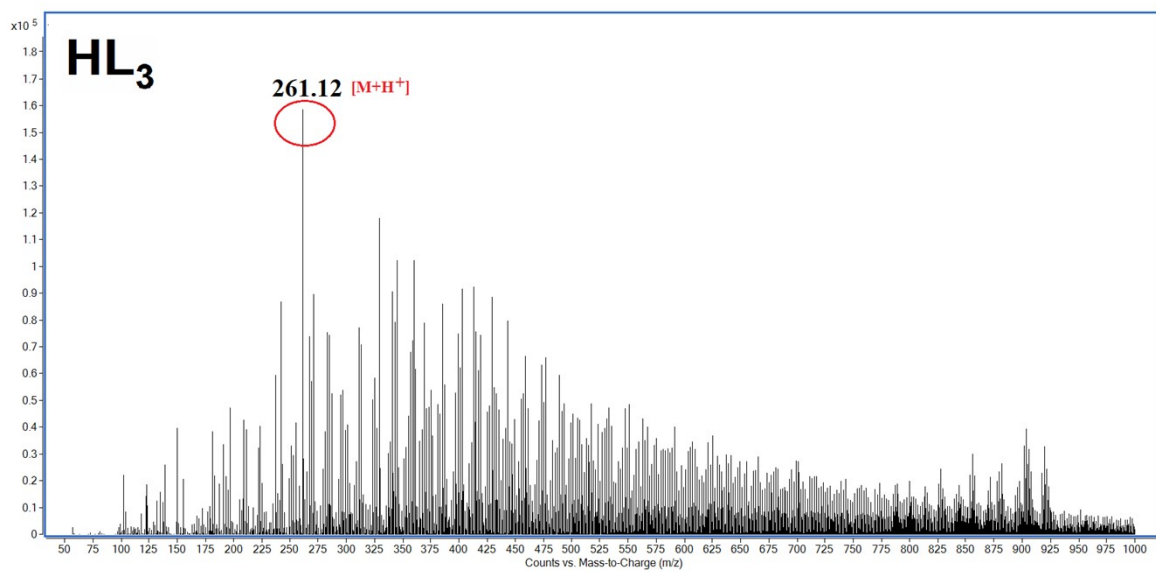


Fig. S11. ESI-MS spectrum of HL₃.

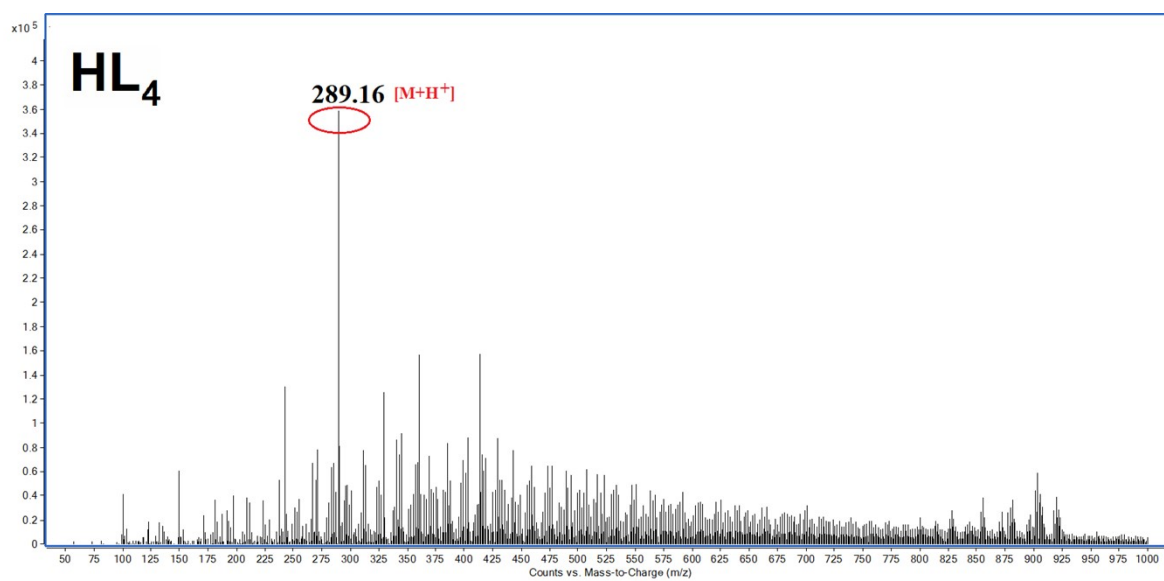


Fig. S12. ESI-MS spectrum of HL₄.

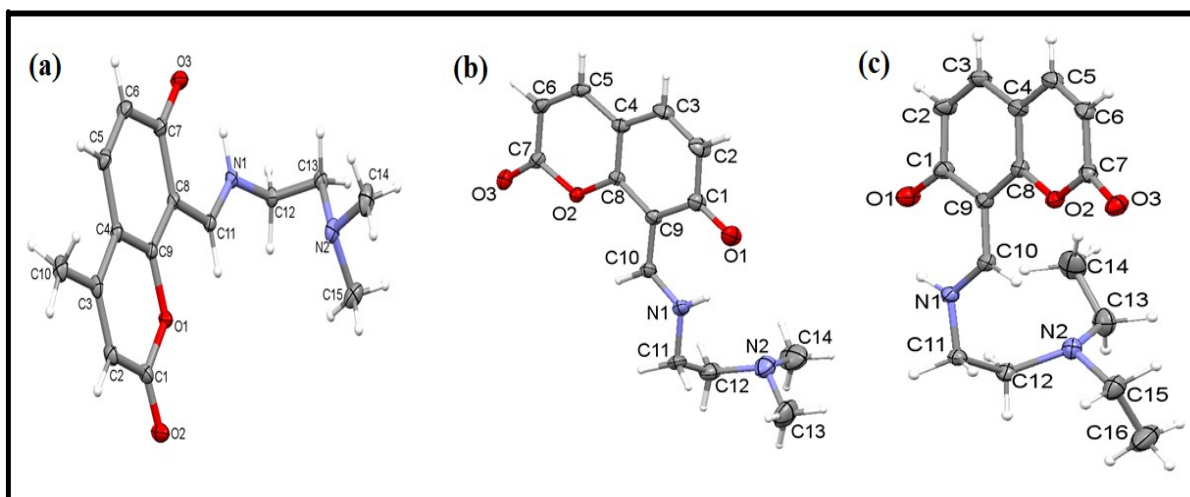


Fig. S13. ORTEP view of (a) HL₁, (b) HL₃, and (c) HL₄. The ellipsoids represent a 50 % probability level displacement.

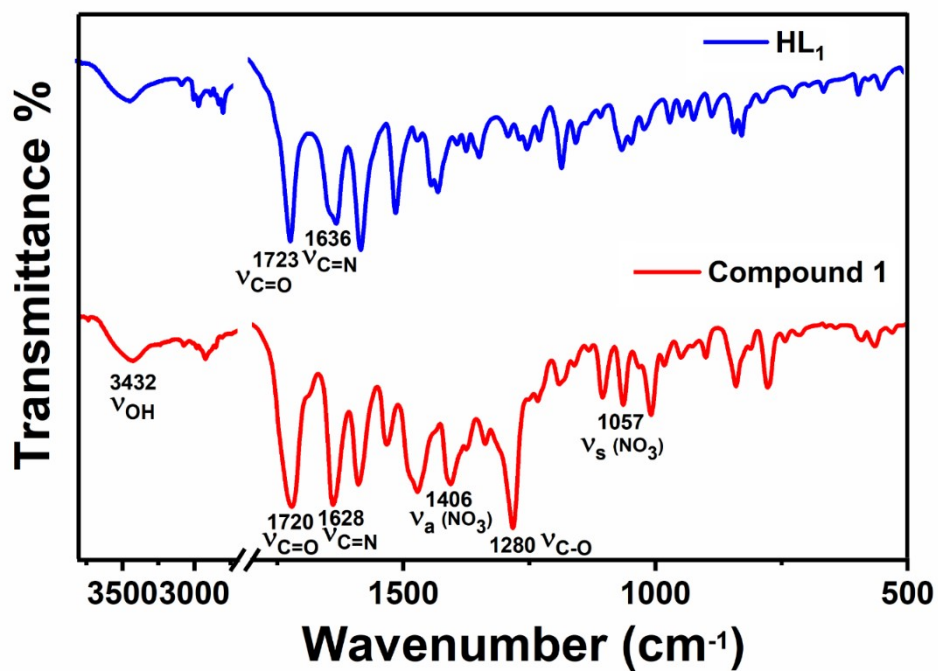


Fig. S14. FT-IR spectra of HL₁ (top panel) and its Cu-complex 1 (bottom panel).

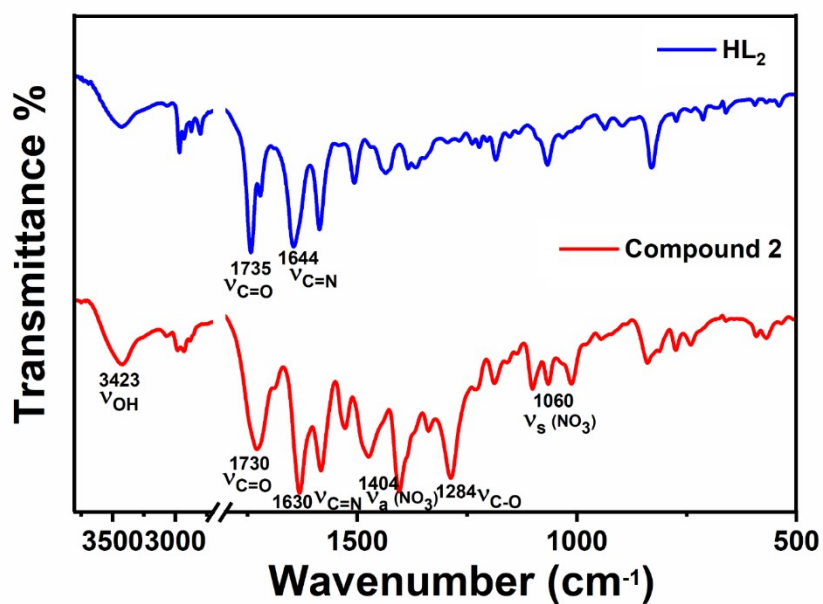


Fig. S15. FT-IR spectra of HL₂ (top panel) and its Cu-complex 2 (bottom panel).

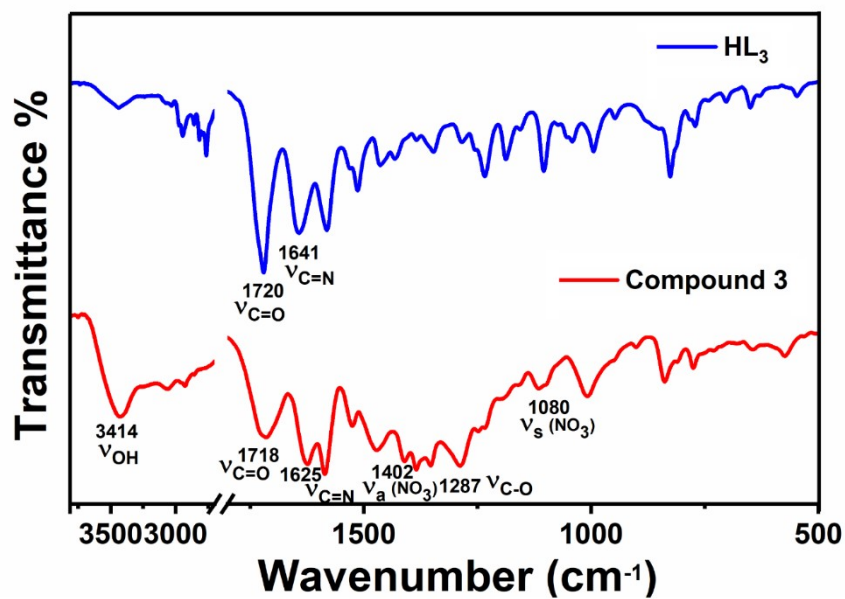


Fig. S16. FT-IR spectra of HL₃ (top panel) and its Cu-complex 3 (bottom panel).

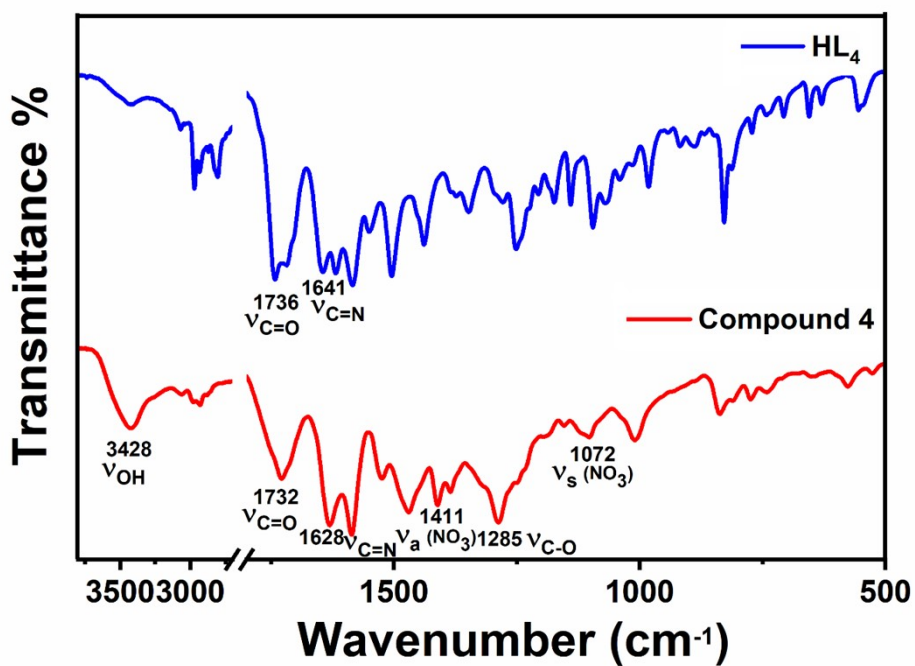


Fig. S17. FT-IR spectra of HL₄ (top panel) and its Cu complex 4 (bottom panel).

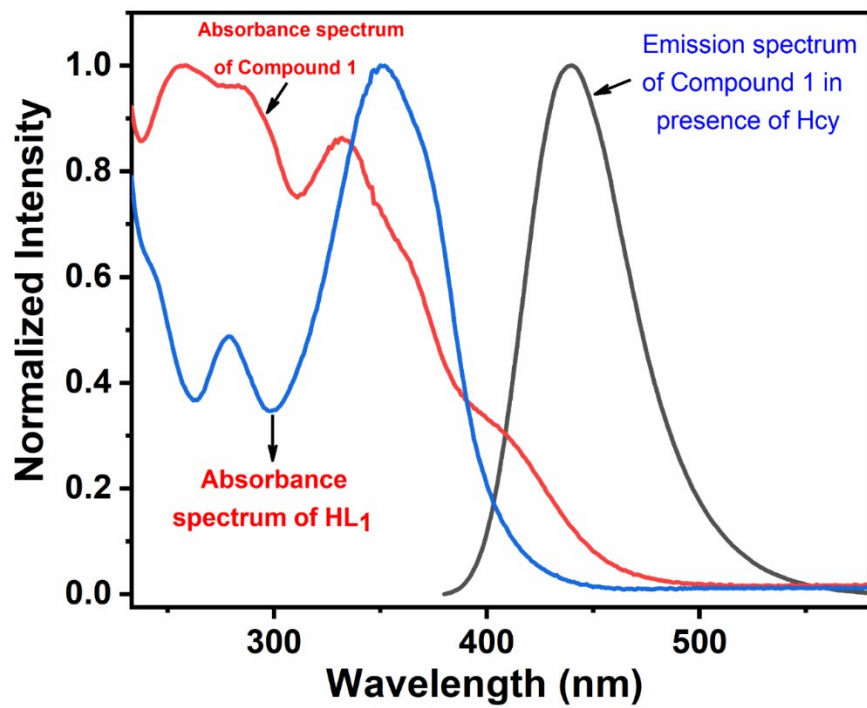


Fig. S18. Absorption spectra of HL₁ and its Cu-compound 1. Emission spectrum of 1 in presence of Hcy ($\lambda_{\text{ex}}=370$ nm).

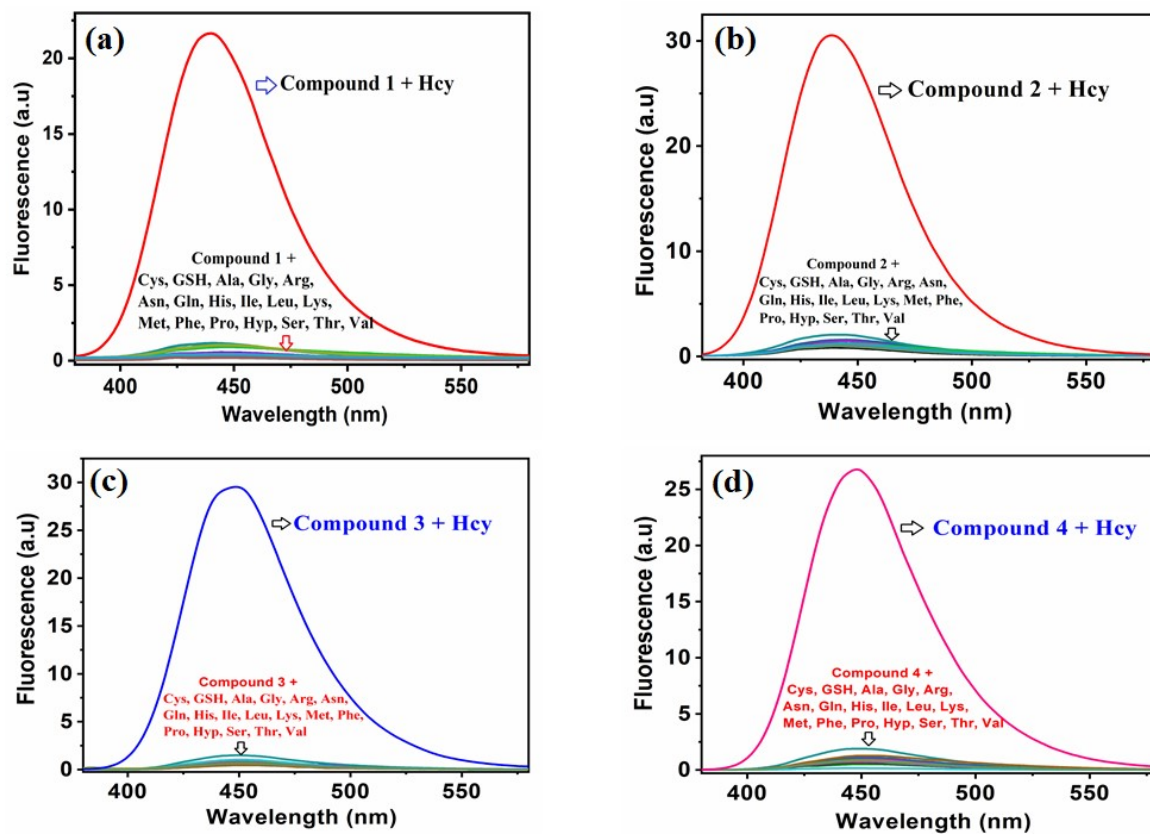


Fig. S19. Fluorescence emission spectra of 1-4 in presence of amino acids in HEPES buffer solution (10 mM, pH = 7.4). Excitation was set at 370 nm.

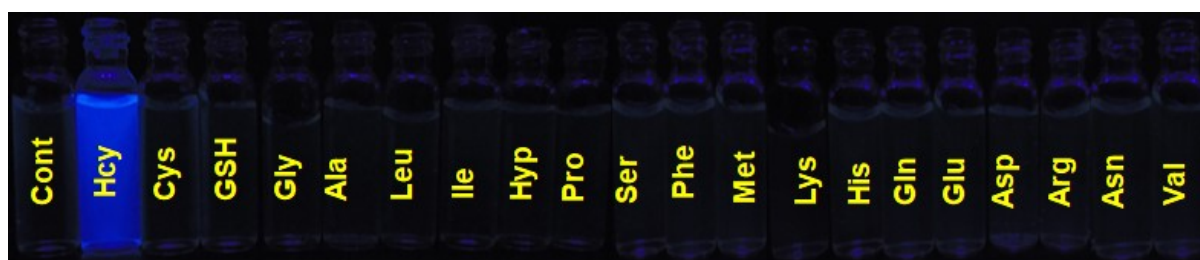


Fig. S20. Photograph showing selective fluorescence response of 1 towards Hcy in presence of different molecules when illuminated with a 365 nm hand held UV lamp.

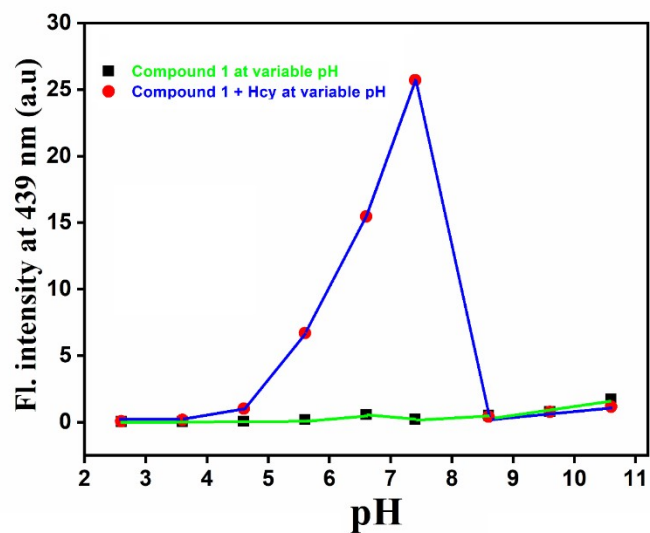


Fig. 21. Change in fluorescence peak intensities of 1 in presence (blue line) and absence (green line) of Hcy with variable pH condition (2.6-10.6). $\lambda_{\text{ex}} = 370 \text{ nm}$ and $\lambda_{\text{em}} = 439 \text{ nm}$.

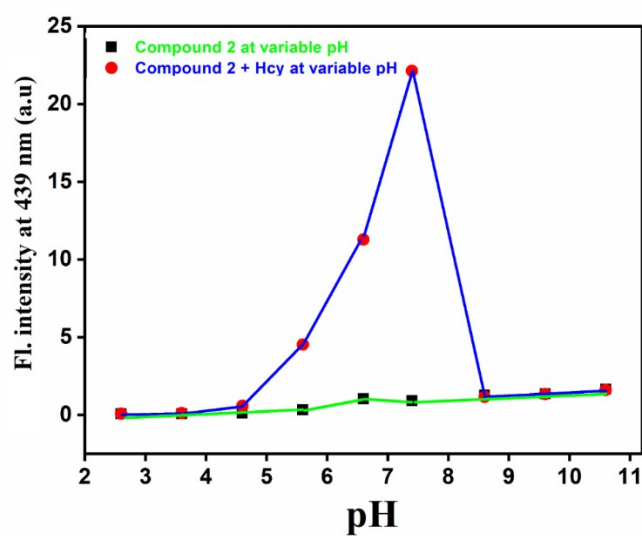


Fig. S22. Change in fluorescence peak intensities of 2 in presence (blue line) and absence (green line) of Hcy with variable pH condition (2.6-10.6). $\lambda_{\text{ex}} = 370 \text{ nm}$ and $\lambda_{\text{em}} = 439 \text{ nm}$.

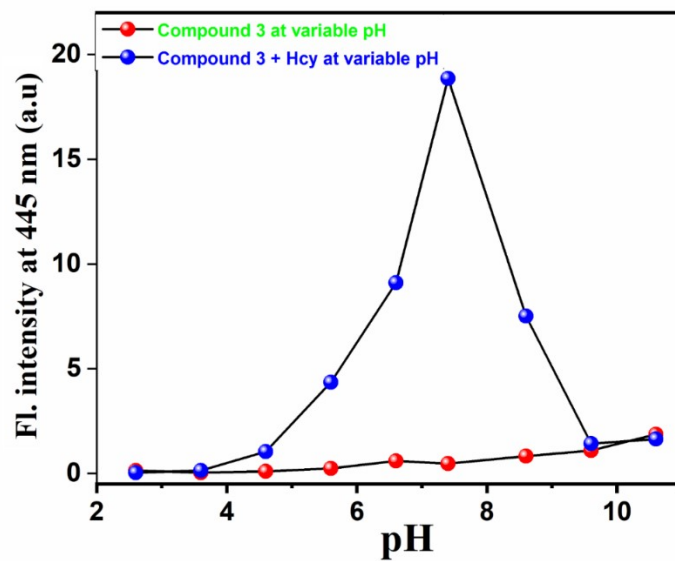


Fig. S23. Change in fluorescence peak intensities of 3 in presence (blue) and absence (red) of Hcy with variable pH solution (2.6-10.6). $\lambda_{\text{ex}} = 370 \text{ nm}$ and $\lambda_{\text{em}} = 439 \text{ nm}$.

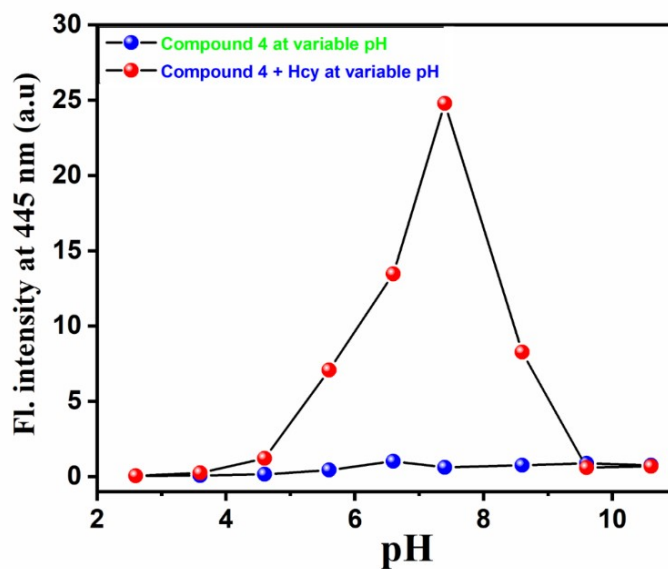


Fig. S24. Change in fluorescence peak intensities of 4 in presence (red) and absence (blue) of Hcy with variable pH solution (2.6-10.6). $\lambda_{\text{ex}} = 370 \text{ nm}$ and $\lambda_{\text{em}} = 439 \text{ nm}$.

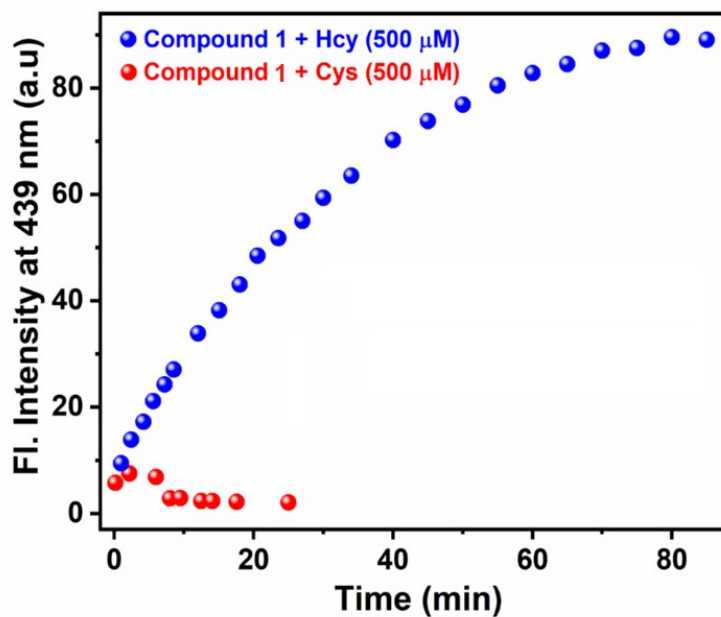


Fig. S25. Time-dependent fluorescence intensity changes of 1 (20 μM) towards 25 equivalents of Hcy (blue) and Cys (red), respectively, in HEPES buffer solution (10 mM, pH = 7.4). λ_{ex} = 370 nm and λ_{em} = 439 nm.

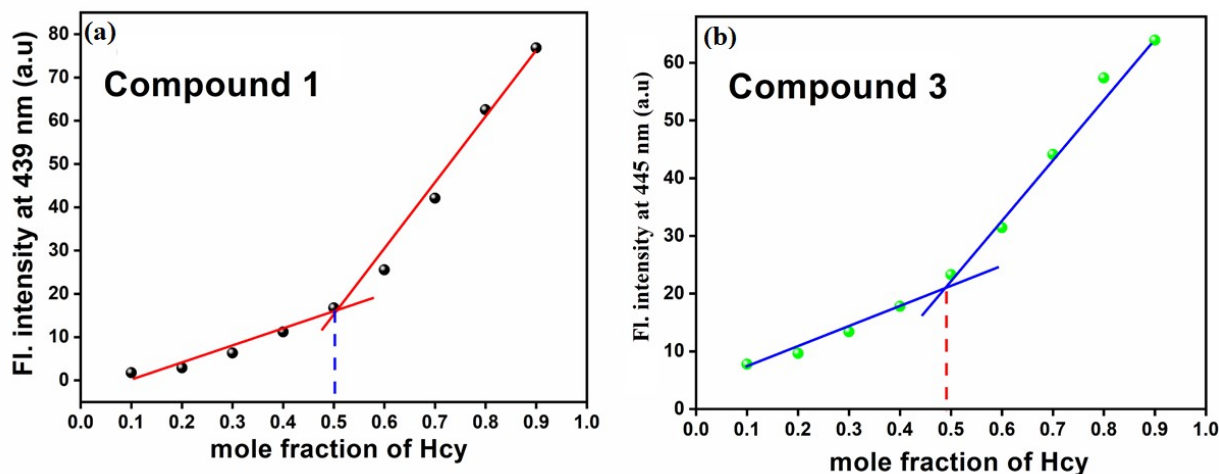


Fig. S26. Job's plots of 1 and 3 monitored at 439 nm and 445 nm (emission), respectively, showing 1:1 binding stoichiometry with Hcy in 10 mM HEPES buffer solution (pH 7.4). Excitation was at 370 nm.

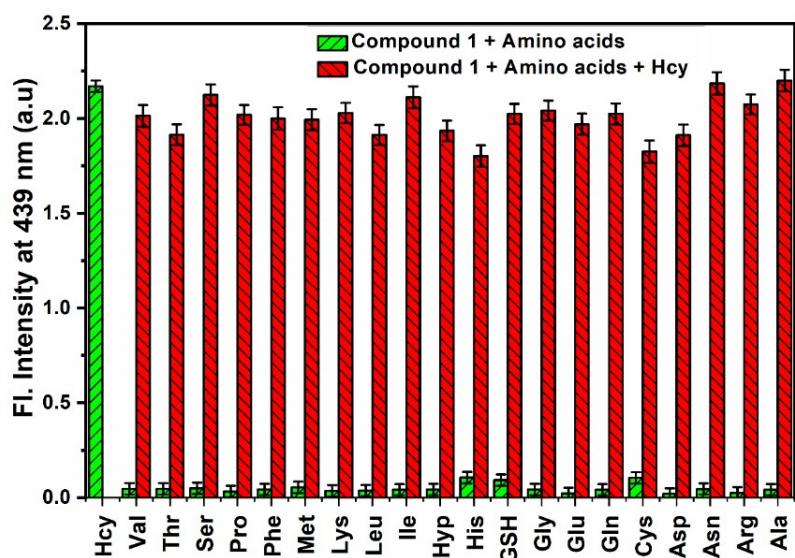


Fig. S27. Bar diagram showing selective fluorescence off-to-on response of 1 (20 μ M in 10 mM, HEPES buffer solution) with Hcy in presence of equivalent amount of other competing amino acids. Excitation was set at 370 nm.

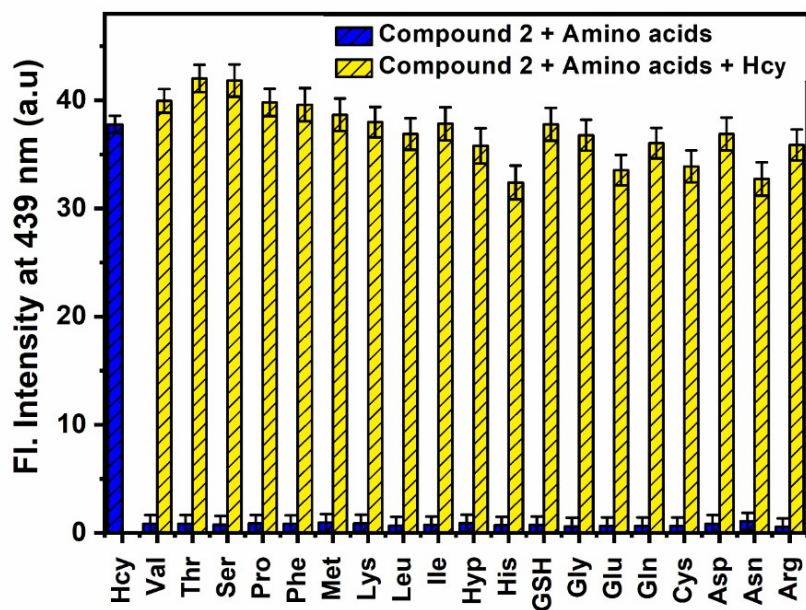


Fig. S28. Bar diagram showing selective fluorescence off-to-on response of 2 (20 μ M in 10 mM, HEPES buffer solution) with Hcy (25 equivalent) in presence of equivalent amount of other competing amino acids. $\lambda_{\text{ex}} = 370$ nm, $\lambda_{\text{em}} = 439$ nm.

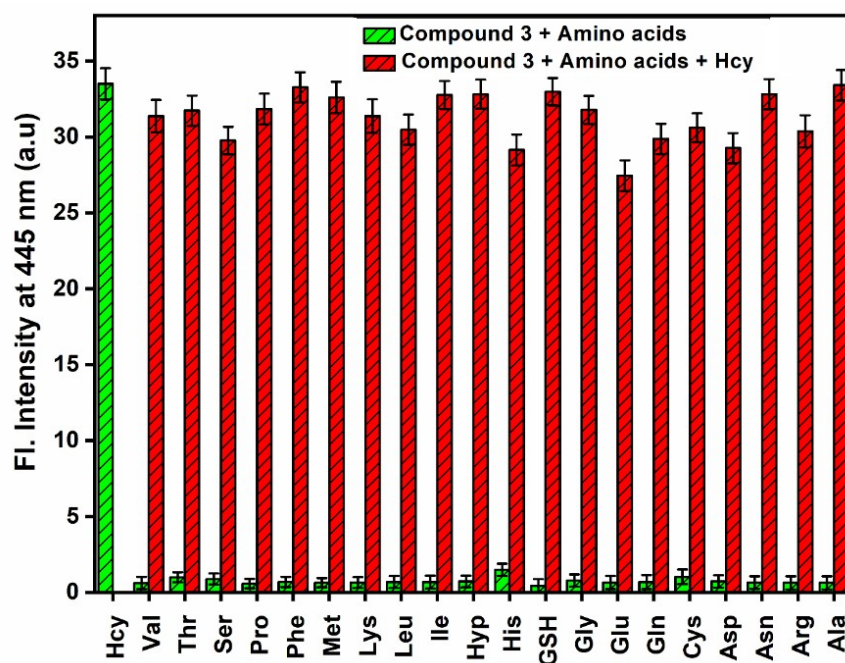


Fig. S29. Bar diagram showing selective fluorescence off-to-on response of 3 (20 μ M in 10 mM, HEPES buffer solution) with Hcy (25 equivalent) in presence of equivalent amount of other competing amino acids. $\lambda_{\text{ex}} = 370$ nm, $\lambda_{\text{em}} = 445$ nm.

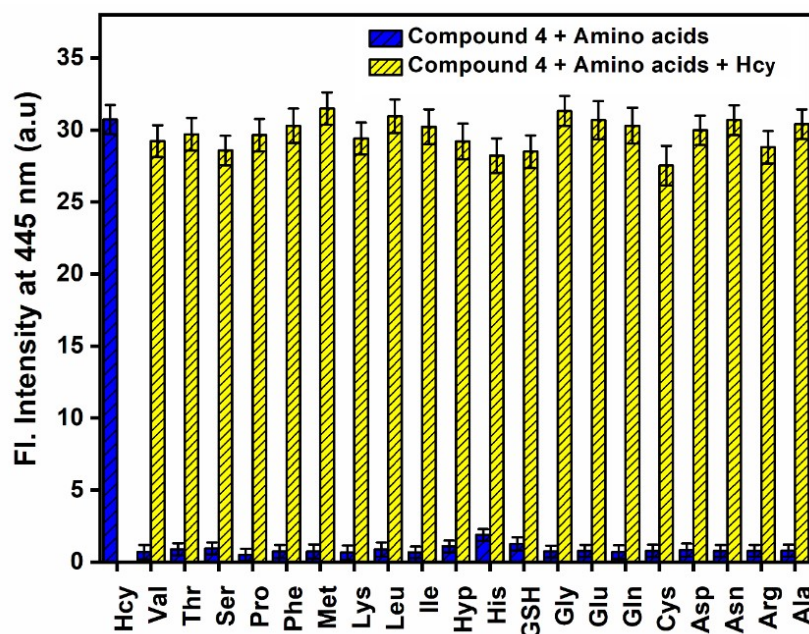


Fig. S30. Bar diagram showing selective fluorescence off-to-on response of 4 (20 μ M in 10 mM, HEPES buffer solution) with Hcy (25 equivalent) in presence of equivalent amount of other competing amino acids. $\lambda_{\text{ex}} = 370$ nm, $\lambda_{\text{em}} = 445$ nm.

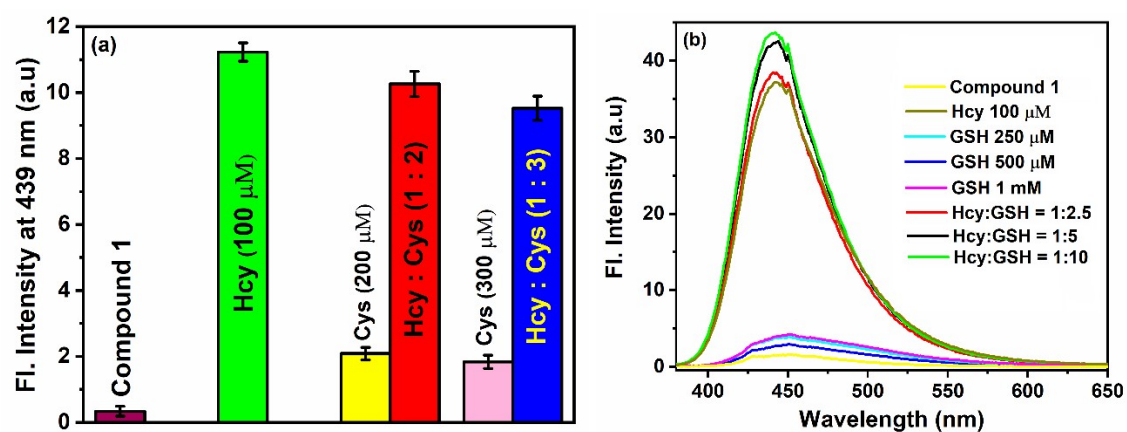


Fig. S31. Interference of varying concentrations of Cys (left, a) and GSH (right, b) during the detection with Hcy by 1 at physiological pH (7.4) in HEPES buffer solution.

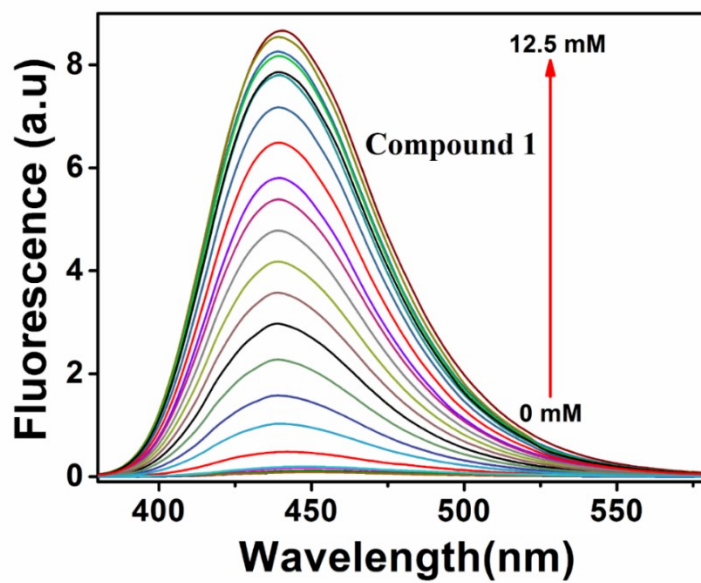


Fig. S32. Fluorescence titration profile of 1 (20 μ M) upon incremental addition of Hcy concentration HEPES buffer solution (pH 7.4).

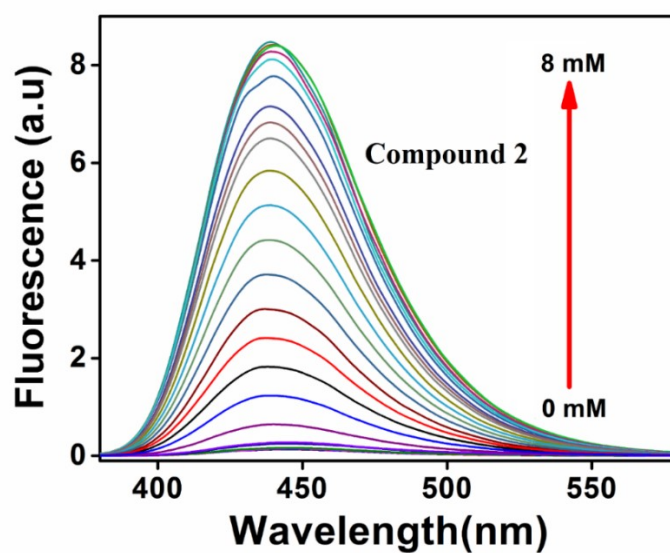


Fig. S33. Fluorescence titration profile of 2 (20 μ M) upon incremental addition of Hcy concentration HEPES buffer solution (pH 7.4).

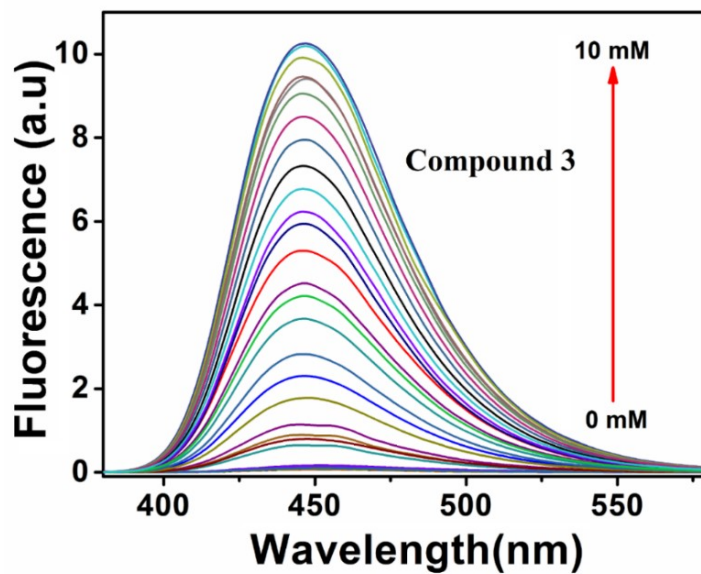


Fig. S34. Fluorescence titration profile of 3 (20 μ M) upon incremental addition of Hcy concentration HEPES buffer solution (pH 7.4).

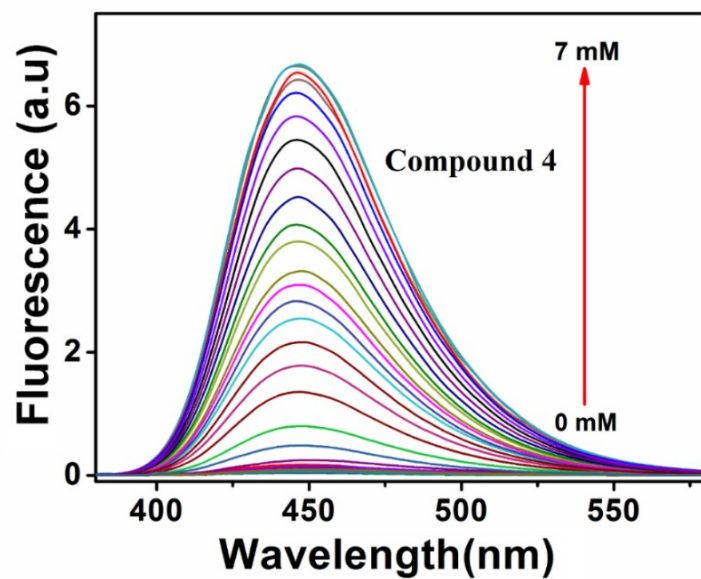


Fig. S35. Fluorescence titration profile of 4 (20 μ M) upon incremental addition of Hcy concentration HEPES buffer solution (pH 7.4).

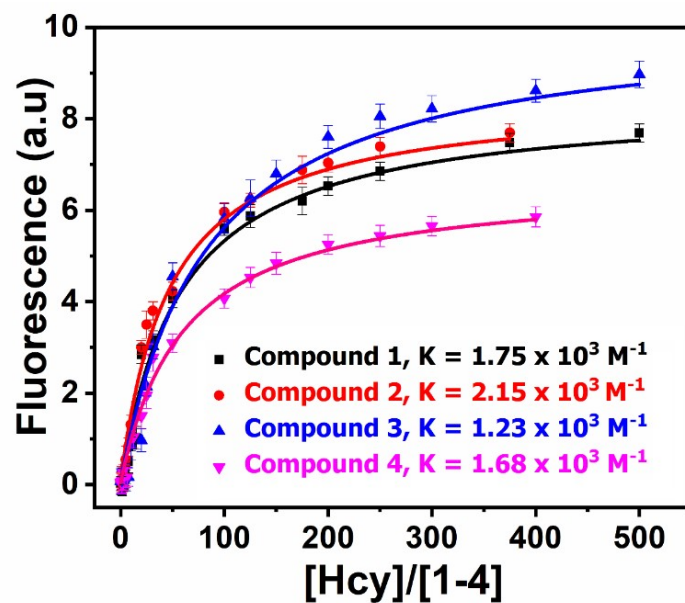


Fig. S36. Nonlinear fitting of the data points obtained from fluorescence titration of 1-4 in presence of varying concentrations of Hcy. Excitation was at 370 nm in HEPES buffer solution (10 mM) at physiological pH (7.4).

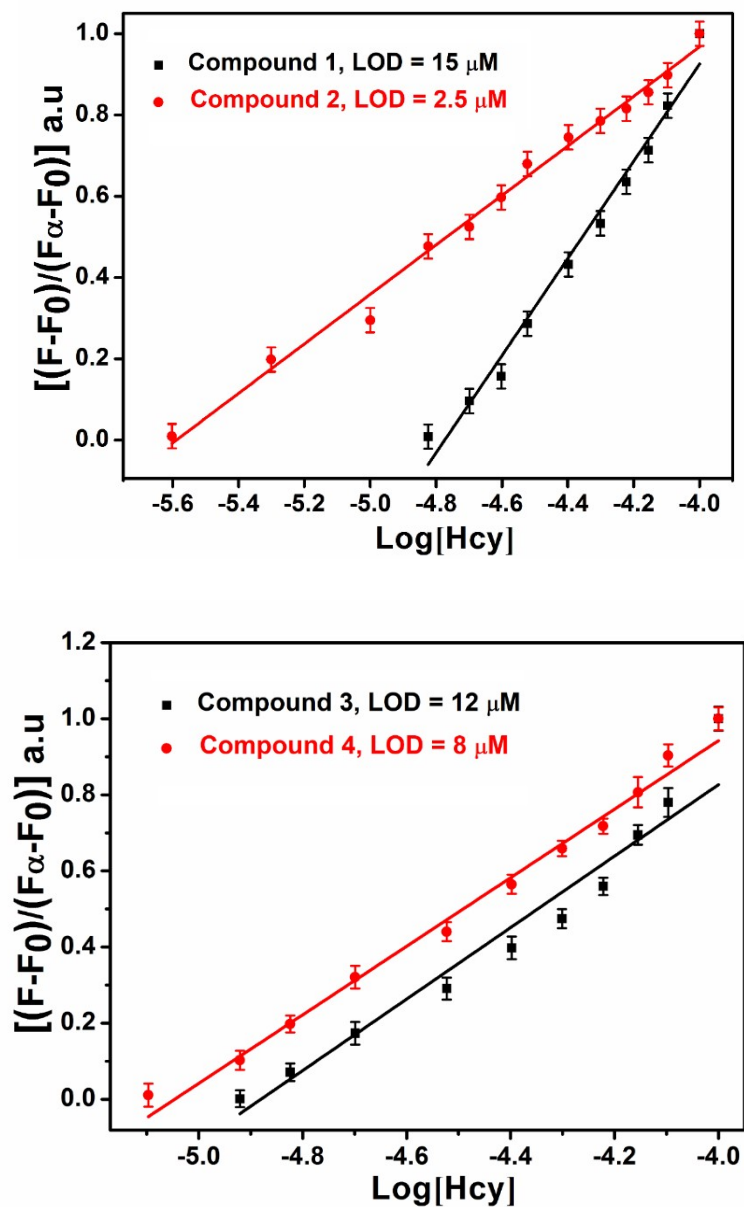


Fig. S37. Limit of detection (LOD) determination plots from fluorescence titration data of 1 and 2 (top panel)/3 and 4 (bottom panel) in presence of different concentrations of Hcy upon excitation at 370 nm in HEPES buffer solution (10 mM) at physiological pH (7.4).

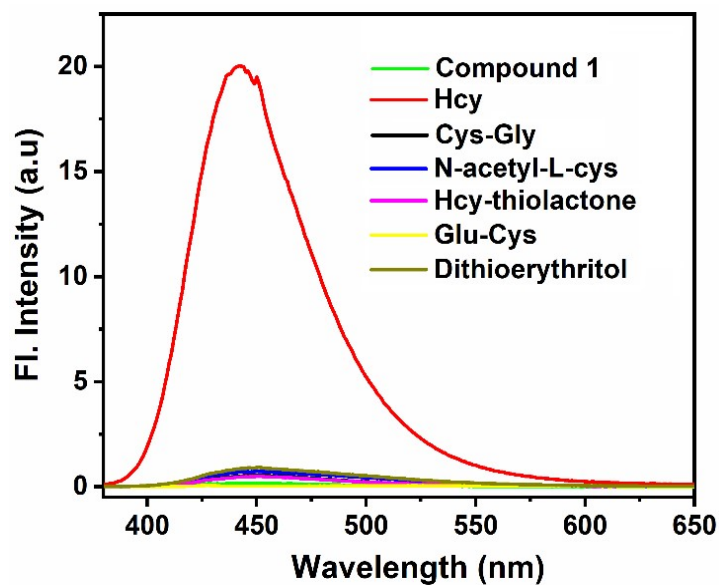


Fig. S38. Fluorescence responses of 1 (20 μM) toward 500 μM of various other thiol containing species.

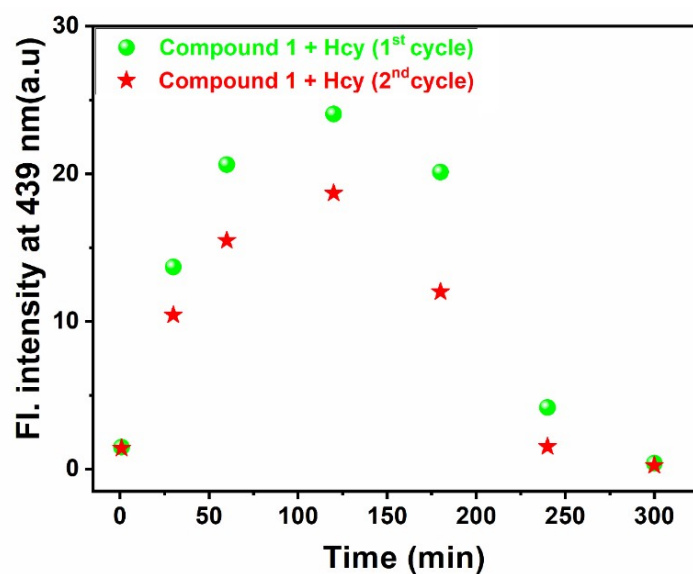


Fig. S39. Time dependent fluorescence responses of 1 (20 μM) at 439 nm in presence of sequential addition of Hcy in HEPES buffer solution (10 mM, pH = 7.4). λ_{ex} = 370 nm.

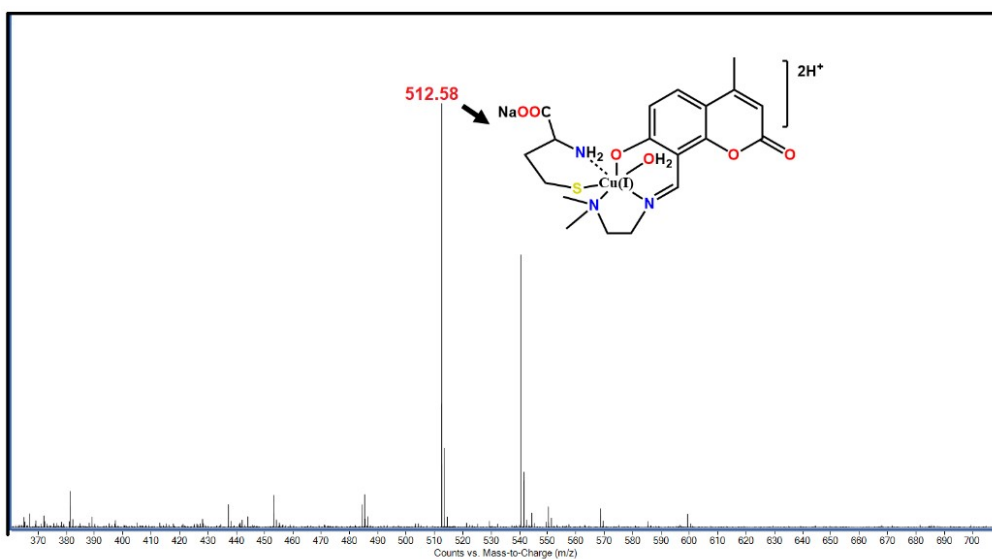


Fig. S40. ESI-MS of 1 in presence of Hcy in water-acetonitrile mixture. The data has been recorded after incubating the mixture of 1 and Hcy for 30 min.

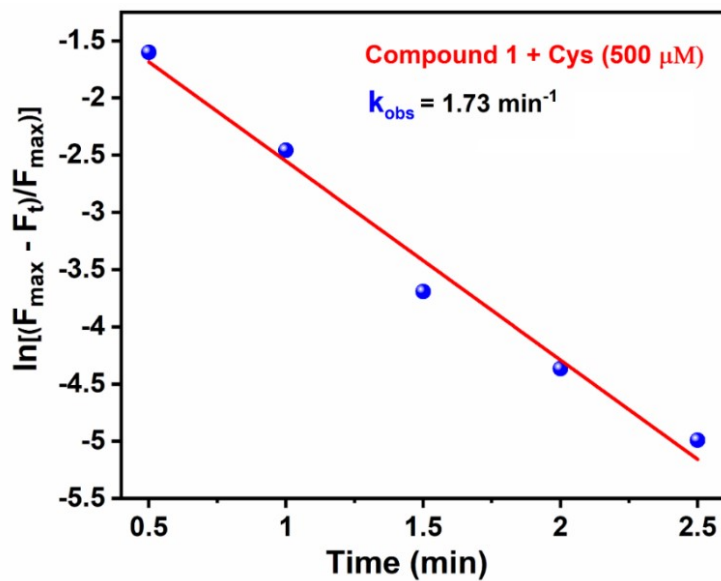


Fig. S41. Pseudo first-order kinetic plot of reaction of 1 (20 μM) with Cys (500 μM) in HEPES buffer solution (10 mM, pH = 7.4) upon excitation at 370 nm.

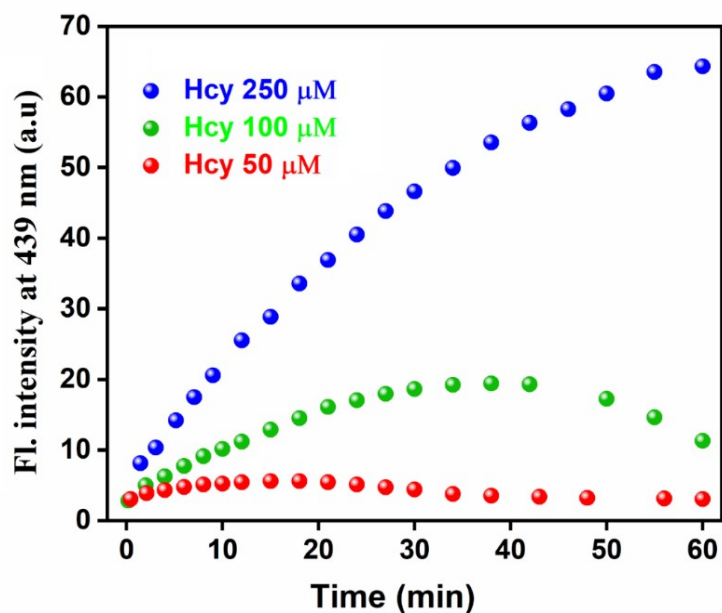


Fig. S42. Time-dependent fluorescence spectral changes of **1** (20 μM) with 250 μM (blue), 100 μM (green), and 50 μM (red) of Hcy, respectively, in 10 mM HEPES buffer solution.

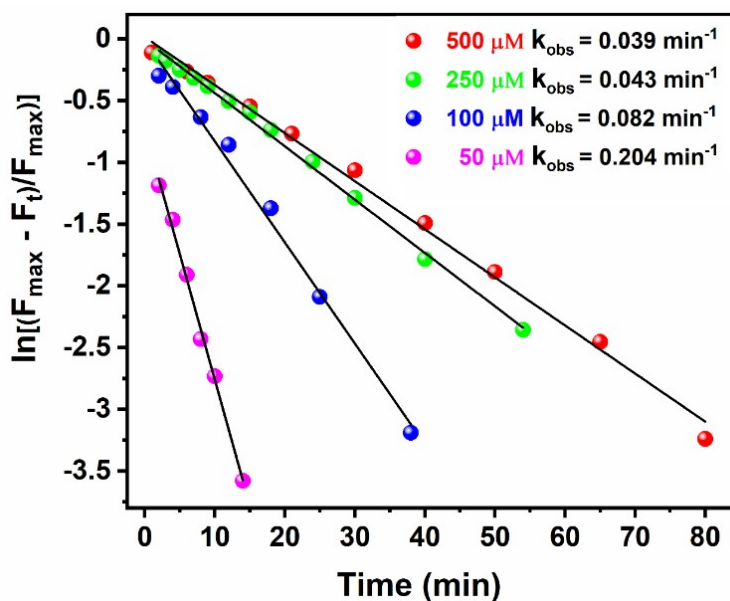


Fig. S43. Pseudo first-order kinetic plots of **1** (20 μM) while reacting with different concentrations of Hcy (50 μM, 125 μM, 250 μM, 500 μM) in HEPES buffer solution (10 mM, pH = 7.4) at 370 nm excitation.

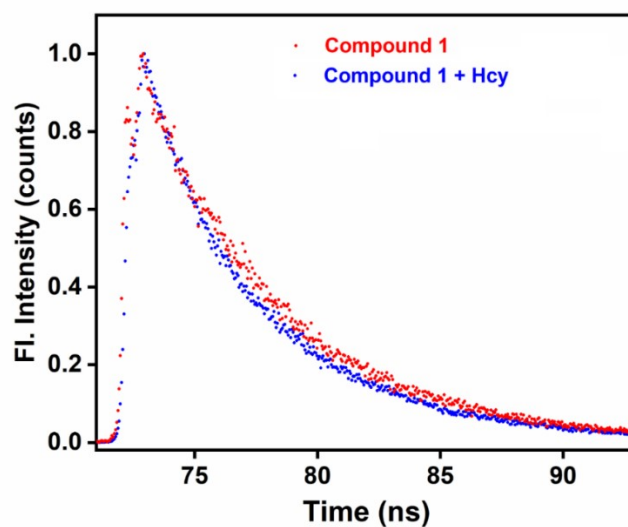


Fig. S44. Time-resolved fluorescence decay of 1 (20 μ M) in absence and presence of 25 equivalents Hcy in HEPES buffer solution. LED excitation at 375 nm was used.

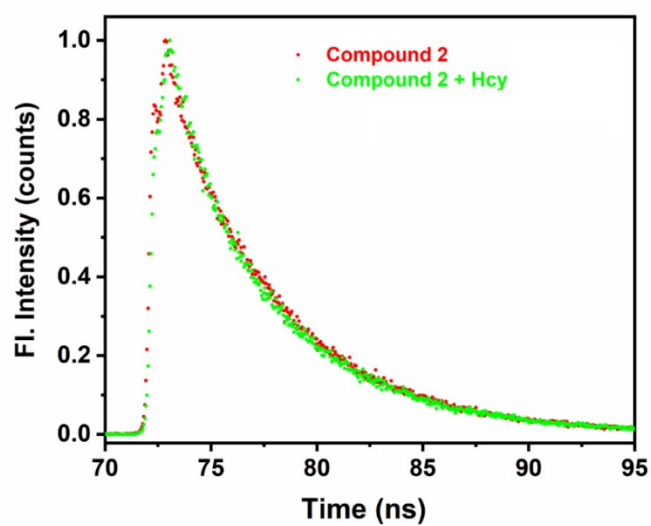


Fig. S45. Time-resolved fluorescence decay of 2 (20 μ M) in absence and presence of 25 equivalents Hcy in HEPES buffer solution. LED excitation at 375 nm was used.

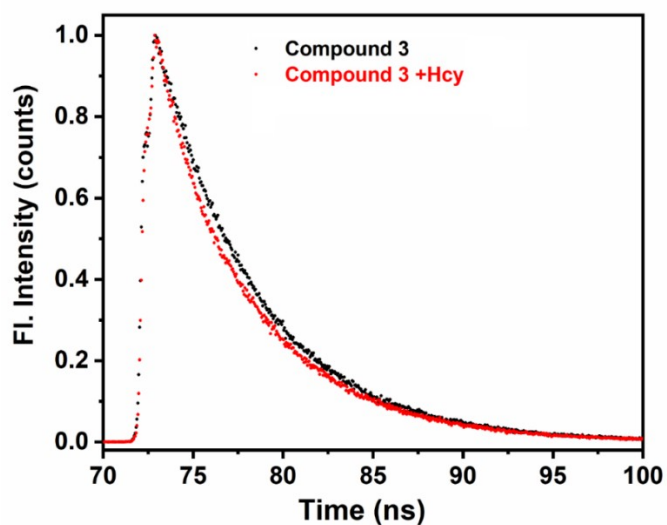


Fig. S46. Time-resolved fluorescence decay of 3 (20 μM) in absence and presence of 25 equivalents Hcy in HEPES buffer solution. LED excitation at 375 nm was used.

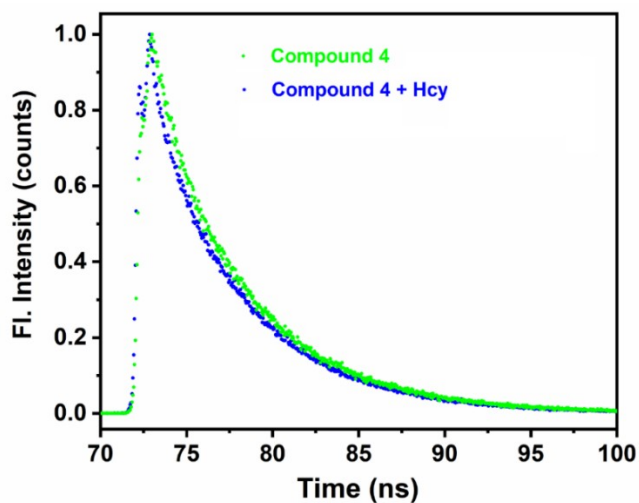


Fig. S47. Time-resolved fluorescence decay of 4 (20 μM) in absence and presence of 25 equivalents Hcy in HEPES buffer solution. LED excitation at 375 nm was used.

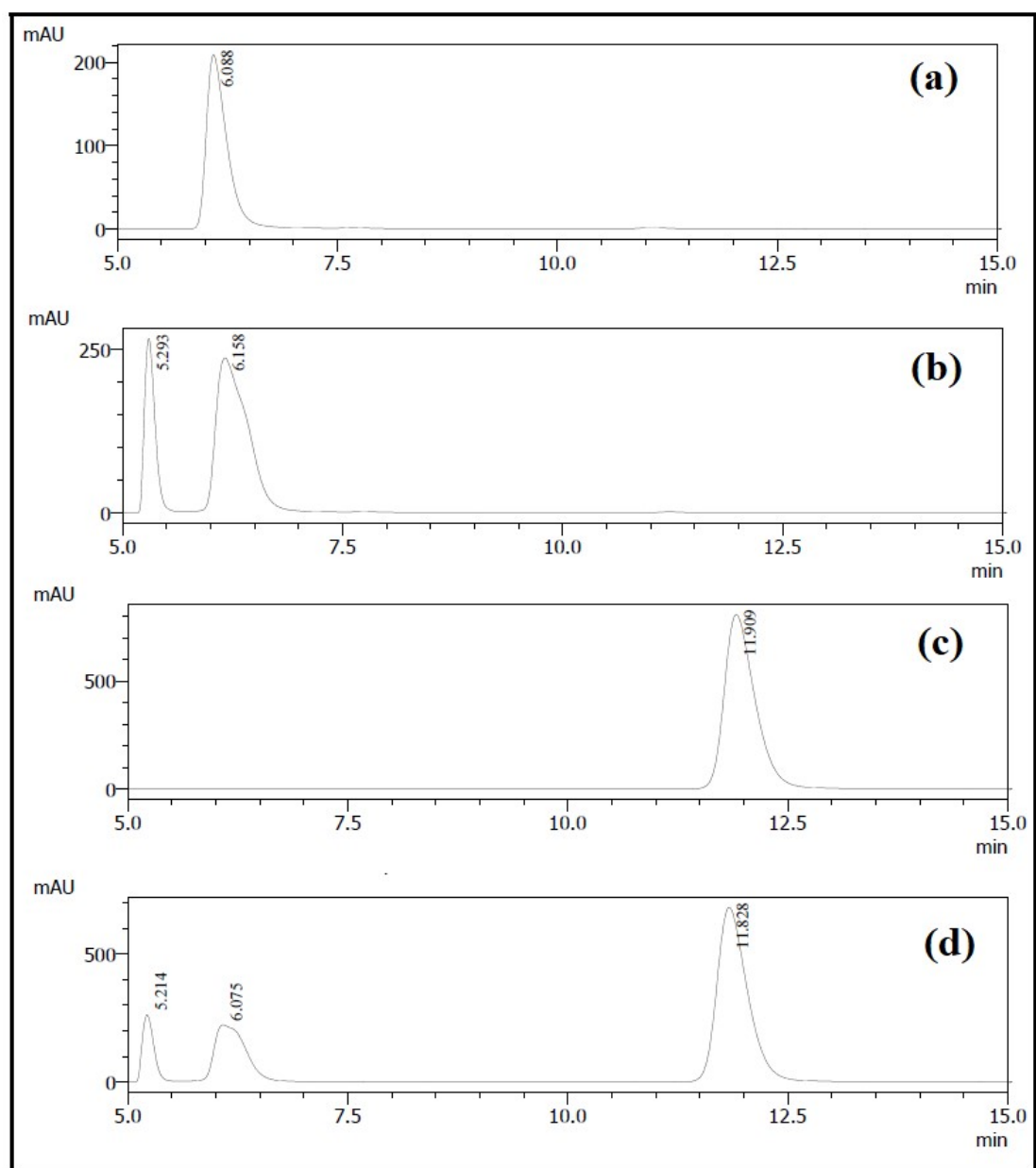


Fig. S48. Comparative HPLC chromatograms of (a) UV labelling reagent only (2-chloro-1-methylpyridinium iodide, CMPI), (b) CMPI + Hcy, (c) internal standard, cysteine-CPPI (2-chloro-1-methylpyridinium iodide), (d) CMPI + Hcy + internal standard.

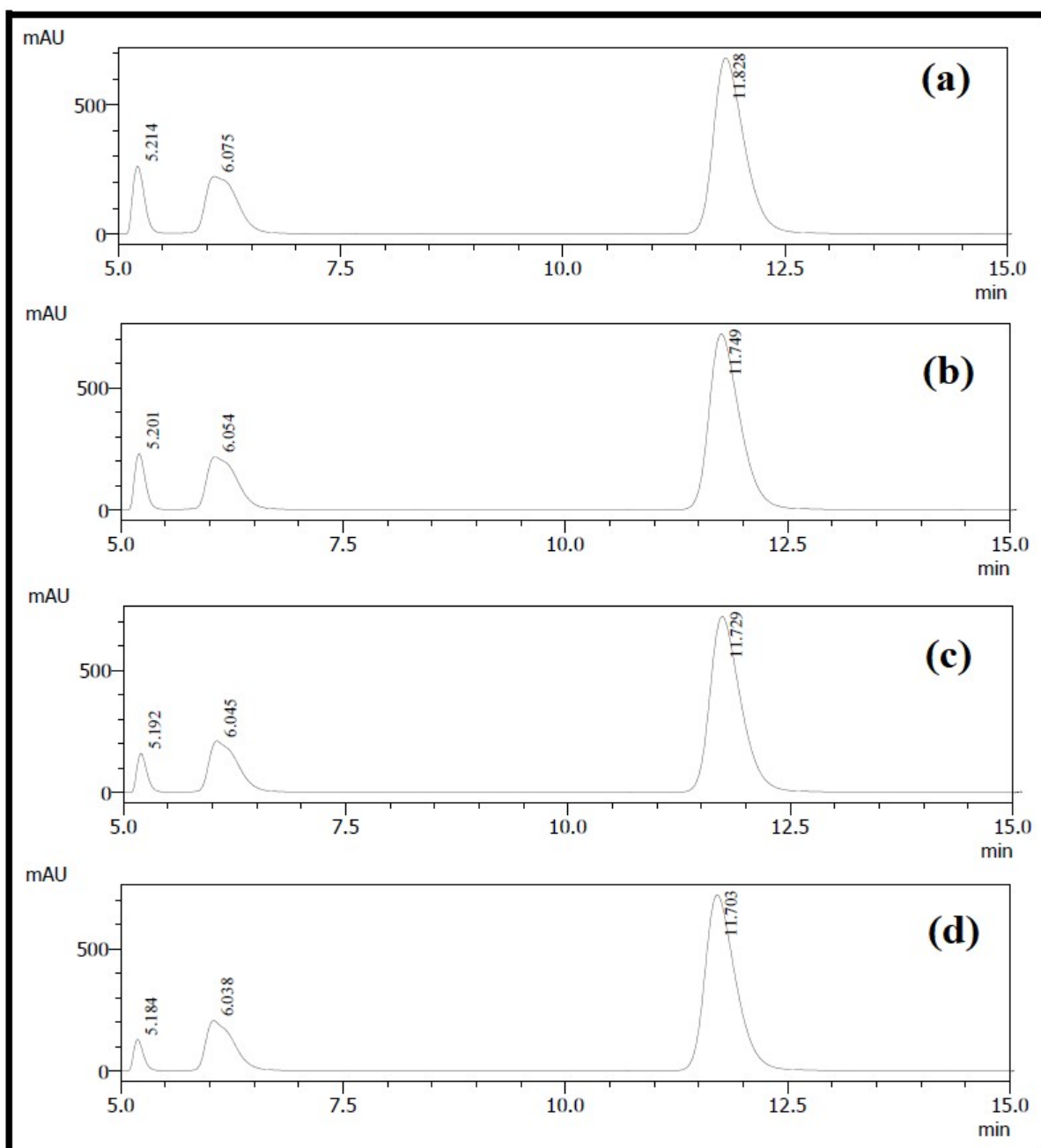


Fig. S49. Comparative HPLC chromatograms showing the reductions in the integrated area of the Hcy-CMPI peak (5.18-5.21 min) with decrease in concentration of Hcy (a) 100 μ M, (b) 80 μ M, (c) 60 μ M, and (d) 40 μ M, respectively.

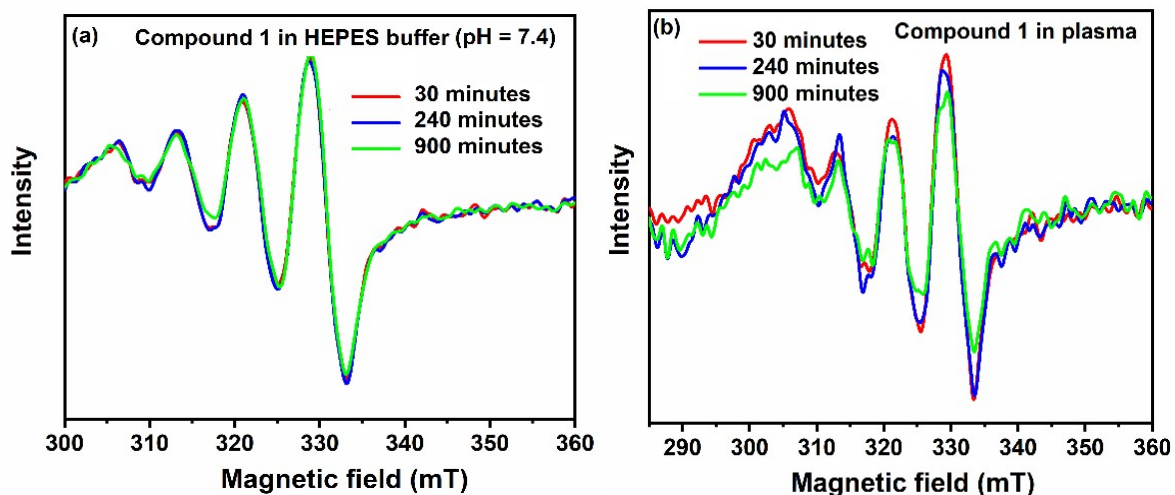


Fig. S50. Kinetic studies of 1 followed by EPR spectroscopy in (a) HEPES buffer (pH = 7.4) and (b) human blood plasma.

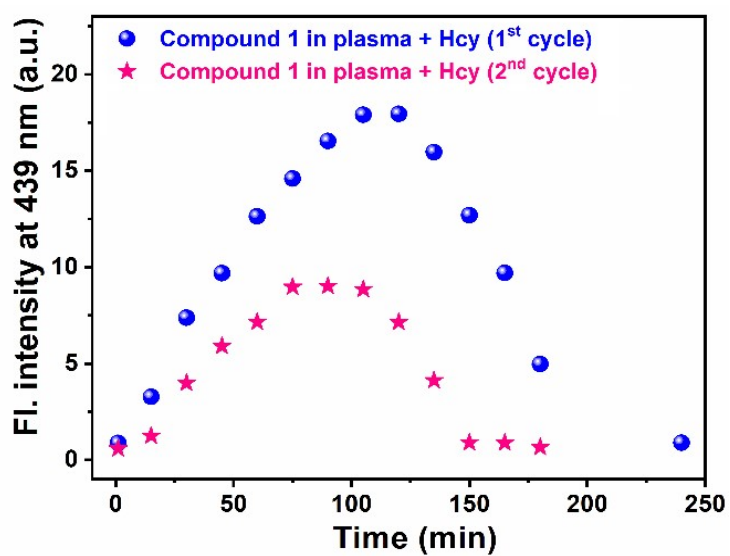


Fig. S51. Time-dependent fluorescence intensity changes of 1 (20 μM) with Hcy (blue) in human blood plasma. $\lambda_{\text{ex}} = 370 \text{ nm}$ and $\lambda_{\text{em}} = 439 \text{ nm}$.

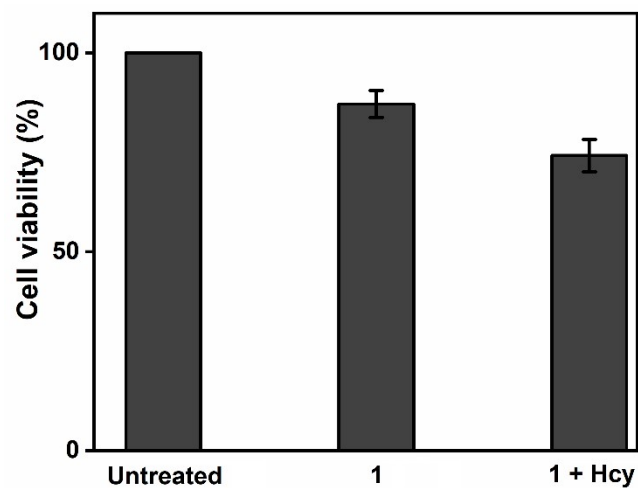


Fig. S52. Cytotoxicity studies of 1 in A549 cells.

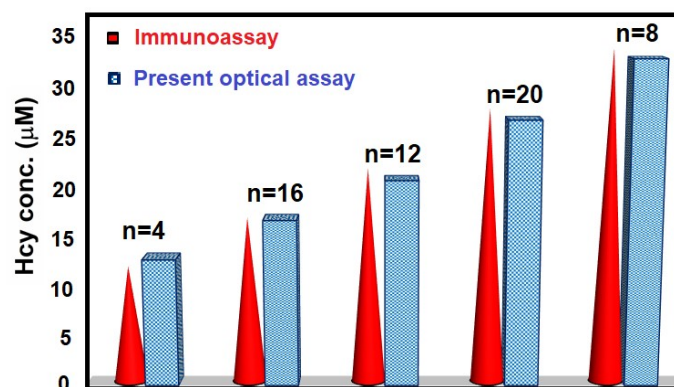


Fig. S53. Validation of 1 with clinically approved immunoassay kit. (“n” represents the number of blood plasma samples tested).

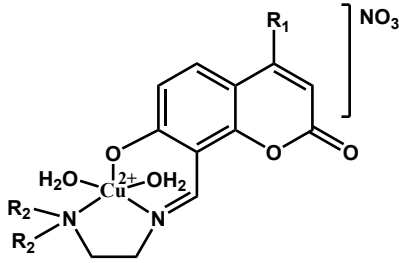
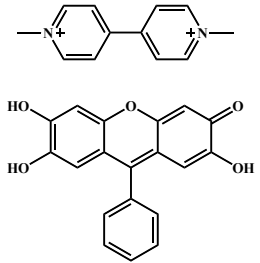
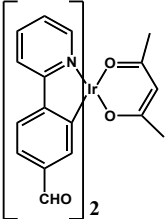
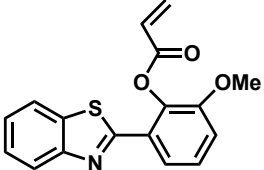
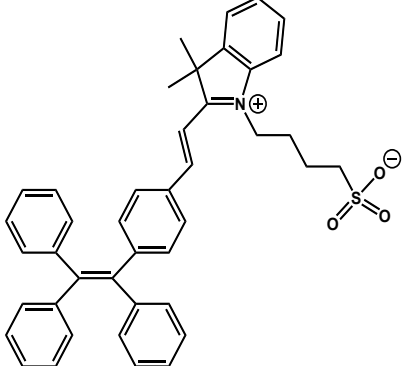
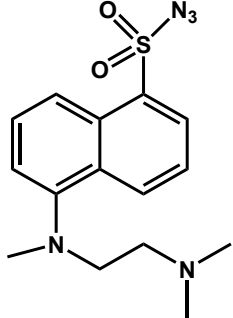
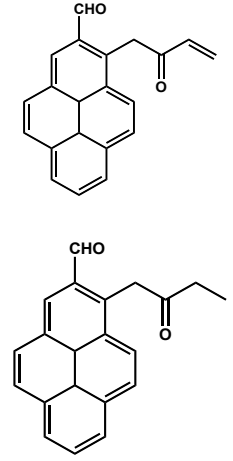
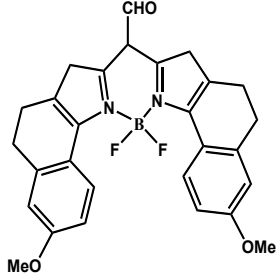
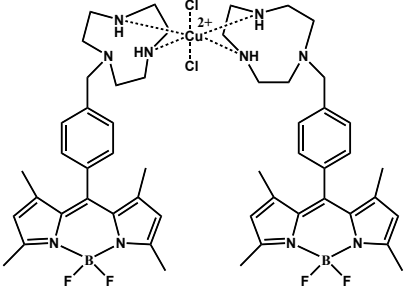
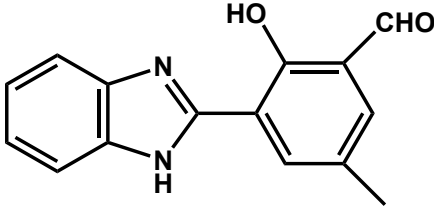
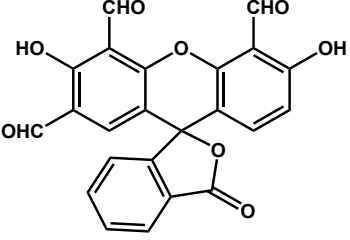
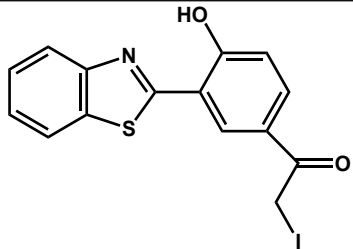
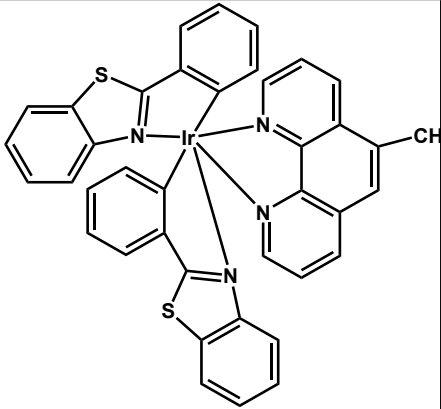
Sl. No.	Probe	Solvent composition	Buffer/pH	Detection technique	Validation	Applications in human plasma	Reference
1		100 % water	7.4 HEPES buffer	Fluorometric Response Turn on	Validation with standard HPLC and clinically approved immunoassay.	Blood plasma from 37 cardiovascular patients and 19 healthy volunteers	Present work
2		100 % water (17 mM aminothiols is required for detection purpose) and 70 % MeOH and 30 % H ₂ O	7.5 Tris buffer and 7.3 phosphate buffer	Colorimetric response	NA	Human Plasma by standard addition method.	9

Table S1. Comparative literature on Hcy selective probes.

3		90 % DMSO and 10 % H ₂ O	7.2 HEPES buffer	Fluorometric (turn on) and colorimetric response	NA	NA	10
4		20 % EtOH and 80 % H ₂ O	7.4 phosphate buffer	Fluorometric response Turn on (ESIPT)	NA	Human plasma sample	11
5		1 % DMSO and 99 % H ₂ O	8 (Ready made buffer solution)	Ratiometric chromo- fluorogenic response	NA	NA	12

6		10 % EtOH and 90 % H ₂ O	7.4 sodium phosphate buffer	Fluorometric response Turn on	NA	Diluted (10 %) fetal bovine serum	13
7		10 % DMSO and 90 % H ₂ O	7.4 HEPES buffer	Fluorometric response. Turn on	NA	NA	14
8		80 % ACN and 20 % H ₂ O	7.2	Fluorometric response. Turn on	NA	NA	15

9		100 % water	7.4 Tris-HCl buffer	Fluorometric response. Turn on	241.4 nM	Human serum of one each of a healthy person and cardiac patient.	16
10		10 % EtOH and 90 % H ₂ O	7.4 HEPES buffer	Fluorometric response. Turn on (ESIPT)	NA	NA	17
11		1 % DMSO and 99 % H ₂ O	6 phosphate buffer	Fluorometric response. Turn on	NA	NA	18

12		1 % ACN and 99 % H ₂ O	7.4 phosphate buffer	Fluorometric response. Turn on	NA	NA	19
13		DMSO was required to dissolve the probe completely	7.4 phosphate buffer	Fluorometric response. Turn on	NA	NA	20

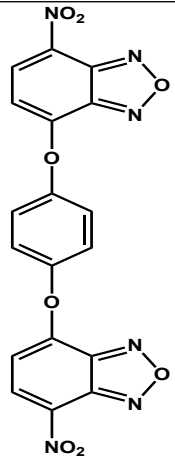
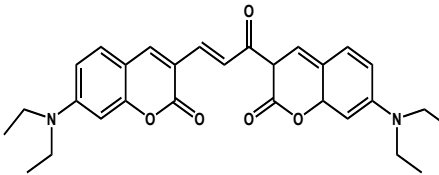
14		30 % DMSO and 70 % H ₂ O	7.4 phosphate buffer	Fluorometric response. Turn on	NA	NA	21
15	Cd-PPCA based MOF	Dispersion	7.4 HEPES buffer	Fluorometric response. Turn on	NA	NA	22
16		50 % DMSO and 50 % H ₂ O	7.4 phosphate buffer	Fluorometric (turn on) and colorimetric response	NA	Spiked Hcy in human blood serum and human urine.	23

Table S2. X-ray crystallographic data of HL₁, HL₃, and HL₄.

Parameters	HL ₁	HL ₃	HL ₄
Molecular formula	C ₁₅ H ₁₈ N ₂ O ₃	C ₁₄ H ₁₆ N ₂ O ₃	C ₁₆ H ₂₀ N ₂ O ₃
Formula weight	274.31	260.29	288.34
Temperature (K)	100 (2)	117 (2)	113 (2)
Crystal system	Triclinic	Monoclinic	Monoclinic
Space group	P-1	P ₂ ₁ /c	P ₂ ₁ /c
Crystal colour	Brown	Yellow	Brown
a (Å)	7.9174 (3)	24.1002 (10)	11.661 (2)
b (Å)	8.2811 (3)	7.6010 (3)	24.120 (5)
c (Å)	11.2569 (5)	6.9925 (3)	10.644 (2)
α (°)	73.486 (10)	90	90
β (°)	72.566 (10)	95.323 (2)	103.846 (13)
γ (°)	83.895 (2)	90	90
Volume (Å ³)	674.92 (5)	1275.40 (9)	2906.8 (11)
Z	2	4	8
Density (g/m ³)	1.350	1.350	1.318
μ mm ⁻¹	0.095	0.096	0.092
F(000)	292	548	1232
Crystal size (mm ³)	0.6 x 0.380 x 0.3	0.234 x 0.046 x 0.012	0.523 x 0.502 x 0.490
2θ range for data collection	5.394 to 63.022	5.1 to 61.12	4.94 to 56.54
Reflections collected	9015	19598	43570
Independent reflections	4351	3823	7164
R _{int}	0.0256	0.0426	0.0199
R _{sigma}	0.0349	0.0342	0.0132
Data/restraints/parameters	4351/0/188	3823/0/214	7164/0/539
Goodness of fit on F ²	1.040	1.088	1.036
R1(F _o), wR2(F _o) (I ≥ 2 σ(I))	0.0392 0.1096	0.0687 0.1764	0.0393 0.1088

R1(F_0^2), wR2(F_0^2) (all data)	0.0441 0.1146	0.0984 0.1960	0.0428 0.1122
CCDC No.	2105919	2105920	2105921

Table S3. X-ray crystallographic data of compound 1.

Parameters	1
Molecular formula	C ₁₅ H ₂₁ CuN ₃ O ₈
Formula weight	434.90
Temperature (K)	111 (2)
Crystal system	Triclinic
Space group	P-1
Crystal colour	Green
a (Å)	6.5708 (5)
b (Å)	7.9441 (6)
c (Å)	17.2086 (14)
α (°)	100.632 (2)
β (°)	93.802 (2)
γ (°)	96.173 (2)
Volume (Å ³)	874.32 (12)
Z	1
Density (g/m ³)	1.652
μ mm ⁻¹	1.300
F(000)	450
Crystal size (mm ³)	0.640 x 0.162 x 0.074
2θ range for data collection	4.84 to 61.18
Reflections collected	32888
Independent reflections	5371
R _{int}	0.0255
R _{sigma}	0.0167
Data/restraints/parameters	5371/0/328
Goodness of fit on F ²	1.055
R1(F ₀), wR2(F ₀) (I ≥ 2 σ(I))	0.0222 0.0588
R1(F ₀ ²), wR2(F ₀ ²) (all data)	0.0246 0.0605
Largest diffraction peak/hole / e Å ⁻³	0.49/-0.32
CCDC No.	2105918

Table S4. Selected bond distances and bond angles in 1.

Bonds	Bond distances (Å)	Angles	Bond Angles (°)
C1-O1	1.291	O1-Cu1-O8	94.56
Cu1-O1	1.92	O1-Cu1-N1	92.33
Cu1-O4	1.991	O1-Cu1-O4	90.79
Cu1-N1	1.939	O8-Cu1-N1	98.70
Cu1-O8	2.351	O8-Cu1-N2	91.49
Cu1-N2	2.054	O8-Cu1-O4	90.17
O1-C1	1.349(3)	N1-Cu1-N2	85.00
C10-N1	1.287	O4-Cu1-N2	90.96

Table S5. Quantum Yield (Φ_f), lifetime (τ_f), and radiative/total non-radiative rate constant (k_r and k_{nr}) values. χ^2 represents the fitting parameter.

Sample	τ_f [ns]	Φ_f	k_r (10^9 s^{-1})	k_{nr} (10^9 s^{-1})	χ^2
Compound 1	5.58	0.0016	0.0003	0.18	1.055
Compound 1 + Hcy	5.15	0.1133	0.022	0.17	0.989
Compound 1 + Cys	5.49	0.0404	0.007	0.17	1.069
Compound 2	5.23	0.001	0.0002	0.19	1.066
Compound 2 + Hcy	5.15	0.091	0.018	0.18	0.979
Compound 2 + Cys	5.27	0.03	0.006	0.18	1.004
Compound 3	5.55	0.0012	0.0002	0.18	1.024
Compound 3 + Hcy	5.41	0.1337	0.025	0.16	0.980
Compound 3 + Cys	5.49	0.079	0.014	0.17	1.001
Compound 4	5.39	0.0019	0.0003	0.19	1.016
Compound 4 + Hcy	5.33	0.1031	0.02	0.17	1.010
Compound 4 + Cys	5.31	0.04	0.008	0.18	0.998

Table S6. Comparative table of Hcy measurement using standard HPLC method and fluorescence technique using compound 1.

Quantitative analysis of Hcy by compound 1			
Samples	[Hcy] from HPLC technique	[Hcy] from fluorescence technique	Error %
Unknown Sample - 1	24.62 μM	25.12 μM	1.99 %
Unknown Sample - 2	74.46 μM	73.19 μM	1.73 %

Table S7: Estimation of total Hcy levels in clinical samples measured by the ADVIA Centaur XP system using chemiluminescence and fluorescence method using probe 1.

Sl. No.	Amount of homocysteine measured by the ADVIA Centaur XP system (μM)	Amount of homocysteine measured by the fluorescence emission obtained from the probe1-Hcy complex (μM)	Sl. No.	Amount of homocysteine measured by the ADVIA Centaur XP system (μM)	Amount of homocysteine measured by the fluorescence emission obtained from the probe1-Hcy complex (μM)
1	14	15	31	16	15
2	12	13	32	16	17
3	18	18	33	17	16
4	19	18	34	17	16
5	16	16	35	18	19
6	34	34	36	19	21
7	20	19	37	23	23
8	12	12	38	26	27
9	28	30	39	29	30
10	17	17	40	23	23
11	24	26	41	13	14
12	21	21	42	18	19
13	22	21	43	19	20
14	19	20	44	28	29
15	20	18	45	29	30
16	22	22	46	25	24
17	28	27	47	26	28
18	22	20	48	29	30
19	26	28	49	28	29
20	28	27	50	32	33
21	29	30	51	27	28
22	25	27	52	17	17

23	26	27	53	27	27
24	27	29	54	29	30
25	33	31	55	34	33
26	35	33	56	27	29
27	30	31	57	29	31
28	25	27	58	22	23
29	25	26	59	26	26
30	23	24	60	41	42

Notes and references

- 1 G. M. Sheldrick, SADABS, Empirical Absorption Correction Program, University of Göttingen, Göttingen, Germany, 1997.
- 2 G. M. Sheldrick, SAINT 5.1 ed., Siemens Industrial Automation Inc., Madison, WI, 1995.
- 3 G. M. Sheldrick, SHELXTL Reference Manual: Version 5.1, Bruker AXS, Madison, WI, 1997.
- 4 L. J. Farrugia, ORTEP-3 for Windows; University of Glasgow: Glasgow, Scotland, 1997.
- 5 R. R. Nair, S. Debnath, S. Das, P. Wakchaure, B. Ganguly and P. B. Chatterjee, *ACS Appl. Bio Mater.*, 2019, **2**, 2374–2387.
- 6 A. M. Brouwer, *Pure Appl. Chem.*, 2011, **83**, 2213–2228.
- 7 E. Bald, E. Kaniowska, G. Chwatko and R. Glowacki, *Talanta*, 2000, **50**, 1233–1243.
- 8 M. Kamoto, N. Umezawa, N. Kato and T. Higuchi, *Chem. Eur. J.*, 2008, **14**, 8004–8012.
- 9 W. Wang, J. O. Escobedo, C. M. Lawrence and R. M. Strongin, *J. Am. Chem. Soc.*, 2004, **126**, 3400–3401.
- 10 H. Chen, Q. Zhao, Y. Wu, F. Li, H. Yang and T. Yi and C. Huang, *Inorg. Chem.* 2007, **46**, 11075–11081.

- 11 X. Yang, Y. Guo and R. M. Strongin, *Angew. Chemie - Int. Ed.*, 2011, **50**, 10690–10693.
- 12 S. Chen, Y. Hong, J. Liu, N. W. Tseng, Y. Liu, E. Zhao, J. W. Yip Lam and B. Z. Tang, *J. Mater. Chem. B*, 2014, **2**, 3919–3923.
- 13 H. Peng, K. Wang, C. Dai, S. Williamson and B. Wang, *Chem. Commun.*, 2014, **50**, 13668–13671.
- 14 H. Y. Lee, Y. P. Choi, S. Kim, T. Yoon, Z. Guo, S. Lee, K. M. K. Swamy, G. Kim, J. Y. Lee, I. Shin and J. Yoon, *Chem. Commun.*, 2014, **50**, 6967–6969.
- 15 J. Zhang, X. D. Jiang, X. Shao, J. Zhao, Y. Su, D. Xi, H. Yu, S. Yue, L. J. Xiao and W. Zhao, *RSC Adv.*, 2014, **4**, 54080–54083.
- 16 Z. Li, Z. R. Geng, C. Zhang, X. B. Wang and Z. L. Wang, *Biosens. Bioelectron.*, 2015, **72**, 1–9.
- 17 L. Tang, J. Shi, Z. Huang, X. Yan, Q. Zhang, K. Zhong, S. Hou and Y. Bian, *Tetrahedron Lett.*, 2016, **57**, 5227–5231.
- 18 A. Barve, M. Lowry, J. O. Escobedo, J. Thainashmuthu and R. M. Strongin, *J. Fluoresc.* 2016, **26**, 731–737.
- 19 F. Chen, Z. Chen, Y. Sun, H. Liu, D. Han, H. He, X. Zhang and S. Wang, *RSC Adv.*, 2017, **7**, 16387–16391.
- 20 H. Gao, Z. Li, Y. Zhao, H. Qi and C. Zhang, *Sensors Actuators, B Chem.* 2017, **245**, 853–859.
- 21 J. Wang, X. Shao, J. Wang and S. Shao, *Chem. Lett.*, 2017, **46**, 442–445.
- 22 J. Wang, Y. Liu, M. Jiang, Y. Li, L. Xia and P. Wu, *Chem. Commun.*, 2018, **54**, 1004–1007.
- 23 K. P. Wang, S. Xu, Y. Lei, W. J. Zheng, Q. Zhang, S. Chen, H. Y. Hu and Z. Q. Hu, *Talanta*, 2019, **196**, 243–248.